# Study on the Effects of Covering and Adsorption Layers on Immobilizing Arsenic from Hydrothermally Altered Rock

A dissertation submitted in partial fulfilment of the requirements for the degree of Doctorate in Engineering

by

Pawit Tangviroon

Division of Sustainable Resources Engineering

Graduate School of Engineering

Hokkaido University, Sapporo, Japan

2017

## ABSTRACT

Hydrothermally altered rocks are frequently excavated by construction of a number of tunnels located in Hokkaido, Japan. They generally contain substantial amounts of arsenic (As). If the excavated rocks are not disposed properly, As and other contaminants will contaminate the surrounding environments, especially groundwater and soil. A massive amount of hydrothermally altered rock is expected to be produced from the ongoing construction projects of road and railway tunnels. Although landfills specially designed for disposing of the rocks have been constructed, they are economically infeasible and unsustainable. Thus, many researchers have focused on investigating factors controlling the mobility of As from hydrothermally altered rocks to develop a reasonable technique for disposing of these waste rocks. Recently, several studies have investigated the mechanisms of As migration from hydrothermally altered rocks by using laboratory column experiments. In this dissertation, more in-depth study of the mechanisms controlling the movement of As was conducted by focusing on two concerns: (1) developing a method to demonstrate the effects of water content and oxygen ($O_2$) concentration in relation to adding covering and adsorption layers on As leaching by introducing water content and $O_2$ concentration sensors into columns, and (2) modeling of As migration to provide insights into the transport phenomena of As through an adsorption layer by using Hydrus-1D. The results would be further extrapolated for designing and establishing a sustainable technique for disposal of hydrothermally altered rocks. This dissertation contains 5 chapters.

Chapter 1 illustrates a literature review on basic knowledges about As, including general properties, effects on human health, sources specifically in rock-forming minerals, and common technics to remove aqueous As. This chapter also includes the fundamental adsorption theories and general knowledge on modeling of solute migration in a vadose zone. At the end of the chapter, the objectives and outline of the study are introduced.

Chapter 2 describes the effects of water content and $O_2$ concentration in relation to additional layer(s), i.e., surface covering and bottom adsorption layers, on As leaching by using laboratory columns with water content and $O_2$ concentration sensors. The results showed that the use of additional layer(s) had a significant effect on lowering As migration. This was due not only to the adsorption capacity of As by the adsorption layer but also to the water content and $O_2$ concentration inside the rock layer. The accumulation of pore water was increased in the rock layer in cases with additional layer(s), which resulted in lower $O_2$ concentration in the rock layer. Consequently, the leaching of As by the oxidation of As-bearing minerals in the rock layer was reduced. Moreover, a longer water-resident time in the rock layer may induce more precipitation of iron (Fe) oxy-hydroxide/oxide. These results suggest that the

geochemical conditions of the rock layer affect As leaching and migration.

After identifying the effects of the water content and $O_2$ concentration in relation to the additional layer(s) on As migration, simulation of reactive solute transport was conducted to investigate the performance of unsaturated adsorption layer on retarding the As from the hydrothermally altered rocks. Compared to the modeling of As migration under saturated condition, unsaturated condition requires more complicated water flow equations. This, however, leads to more accurate prediction since water movement is an important factor affecting solute migration. Thus, in chapter 3, simulation of water movement in multilayer soil profiles was carried out using Hydrus-1D to evaluate the capability of this software package in simulating the solute migration from column experiments. The assessment of the accuracy of the model was done by comparing the simulated with observed data. The water movement was successfully modeled with the high level of accuracy. Therefore, Hydrus-1D is capable of simulating the reactive solute transport with accurate water movement. The results from this chapter will be used as an input to evaluate the As migration in chapter 4.

In chapter 4, performance of a river sediment on immobilizing As from hydrothermally altered rocks was evaluated using laboratory column experiments and Hydrus-1D. The results revealed that the river sediment significantly reduced As migration. Arsenic retarded by the river sediment occurred in three patterns. The first was an adsorption onto minerals originally contained in the river sediment. The next pattern was a combination of reduction of As generation by oxidation of As bearing-minerals, irreversible adsorption, and adsorption onto newly precipitated Fe oxy-hydroxide/oxide. The last pattern was a depletion in As leaching due to a further reduction of oxidation of sulfide mineral. The observed breakthrough curves of As agreed with the simulated results by considering the above three patterns.

Finally, conclusions as well as tentative design of disposal technique for excavated rock containing high content of As are discussed in chapter 5. The designed structure composes of low permeable covering and adsorption layers on the top and underneath the rock, respectively. In addition, layers of neutralizer should be added to the waste rock, containing high pyrite but low-buffer mineral content.

**TABLE OF CONTENTS**

## LIST OF FIGURES

## LIST OF TABLES

# Chapter 1

# GENERAL INTRODUCTION

## 1.1. Property of Arsenic

Arsenic (As) is a metalloid with an atomic number of 33. It appears in various compounds; metallic grey, yellow and black. The element, itself, has a crystalline solid structure at room temperature and very brittle. It has a smell of garlic in air and can be oxidized to arsenous acid at elevated temperature. Although As and its compounds are extremely toxic (Buchanan 1962; Ferguson and Gavis 1972), it is being used in various industrial applications for various purposes due to its properties. The toxicity of As is beneficial in making pesticides and insecticides for agricultural purpose (Murphy and Aucott 1998). In addition, it is also used to preserve wood products (Rahman et al. 2004), used in glass manufacturers (Environmental Protection Agency U.S.A. 1993), or used in bronzing and pyrotechnics (Cross et al. 1979). The physical properties of As are listed in the table below.

Table 1.1 Physical properties of arsenic

| | |
|---|---|
| Crystal structure | Rhombohedral |
| Atomic radius | 125 pm |
| Atomic mass | 74.9216 |
| Atomic number | 33 |
| Density (293 K) | 5.72 g/cm3 |
| Oxidation states | 5, 3, 0, -3 |
| Melting point | ~817°C |
| Boiling point (sublimation) | 603°C |

Arsenic form can be classified into two types, organic and inorganic. Arsenic combined with carbon and hydrogen is known as organic As. It is found in marine animal and plants such as seaweed (Rose et al. 2007). On the other hand, As combined with at least one other element such as oxygen, chlorine or sulfur but no carbon, is classified as inorganic As. Monomethyl arsenic acid (MAA), dimethyl arsenic acid (DMA), and arseno-sugars are some examples of organic As compounds (Thomas and Bradham 2016). Inorganic As exists in four main oxidation states depending on various environmental factors. The most common oxidation states of inorganic As are +3 (As(III)) and +5 (As(V)). The environmental factors that influence the existence of As in a specific oxidation state in the hydrosphere are, for example, oxidation-reduction reactions, pH conditions, general hydrochemistry, microbial

activity, and other ionic distribution states. Among all of the factors, redox potential and pH contribute the strongest effect to the concentration of As species (Smedley and Kinniburgh 2002).

The Eh-pH diagram for aqueous As species and the distribution of As species as a function of pH are shown in Figs. 1.1 and 1.2, respectively (Brookins 1988; Yan et al. 2000; Ghimire et al. 2003). Arsenite (As(III)) is the dominant form under reducing conditions. While arsenate (As(V)) is a thermodynamically more stable form of As species in well-oxygenated environments. The major As(V) species is $H_2AsO_4$ at a p*K*a of 6.9 and $HAsO_4^-$ at higher pH. Both of the species of As(V) exist at the intermediate region (between pH 6 and 8). At the same time, arsenious acid ($H_3AsO_3$) is the dominant species of As(III) at a p*K*a of pH 9.3. Based on the typical pH of 6 to 8.5 in groundwater, the changing the form of the main As species from As(III) to As(V) anions, specifically $HAsO_4^{2-}$, depend on oxidation conditions.

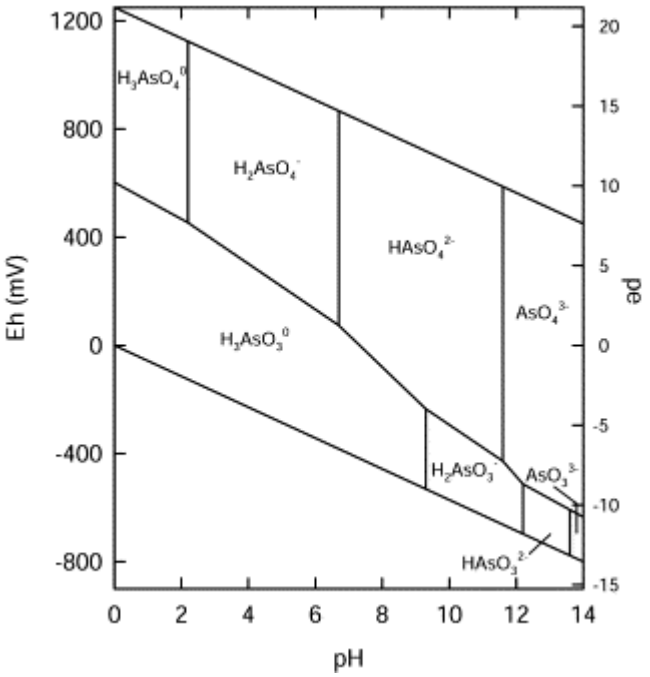


Figure 1.1 Eh-pH diagram of As species for an As-$O_2$-$H_2O$ system at 25 $^{O}$C and 1 bar (Smedley and Kinniburgh, 2002)

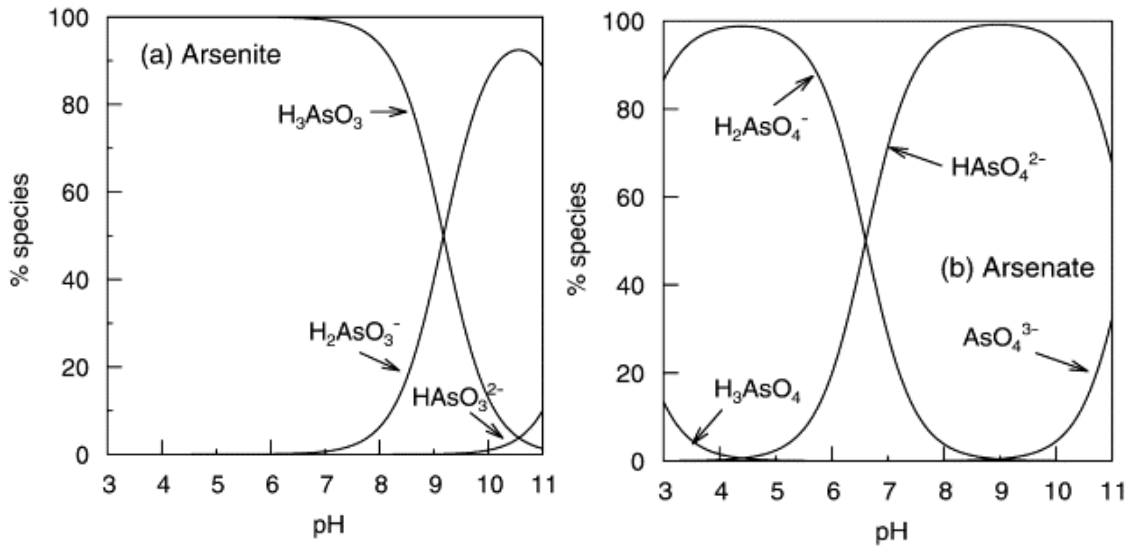


Figure 1.2 Distribution of (a) arsenite and (b) arsenate with pH
(Smedley and Kinniburgh 2002)

## 1.2. **Health Effects**

Generally, organic metal compounds like mercury (Hg) and lead (Pb) have a tendency to be more toxic or damaging than their corresponding inorganic species. Nonetheless, inorganic As compounds have been said to be 100 times more harmful than organic As compounds (Kingston et al. 1993). The toxic level of these species can be ranked as follows: arsenite > arsenate > monomethyl arsenate (MMA) > dimethyl arsenate (DMA) (Penrose 1974; Abdul 2015).

Arsenic exposure causes various kinds of symptoms to many organs in the human body as illustrated in Fig. 1.3 (Abdul 2015). Arsenic toxicity can be divided into acute and chronic toxicity. The major origin of acute As poisoning can be traced back to the contamination of food and drinks. Acute As poisoning develops symptoms such as dryness of mouth and throat and burning sensation along with muscles cramping up. Diarrhea and projectile vomiting are also some of the common symptoms seen in acute As infected individuals (Glazener et al. 1968). On the other hand, symptoms of chronic As poisoning are most likely to associate with the immunological, neurological, cardiovascular and pulmonary elements of the human body. Prolonged contact may lead to hair loss, peeling off of skin along with frail and brittle nails (Hong et al. 2014).

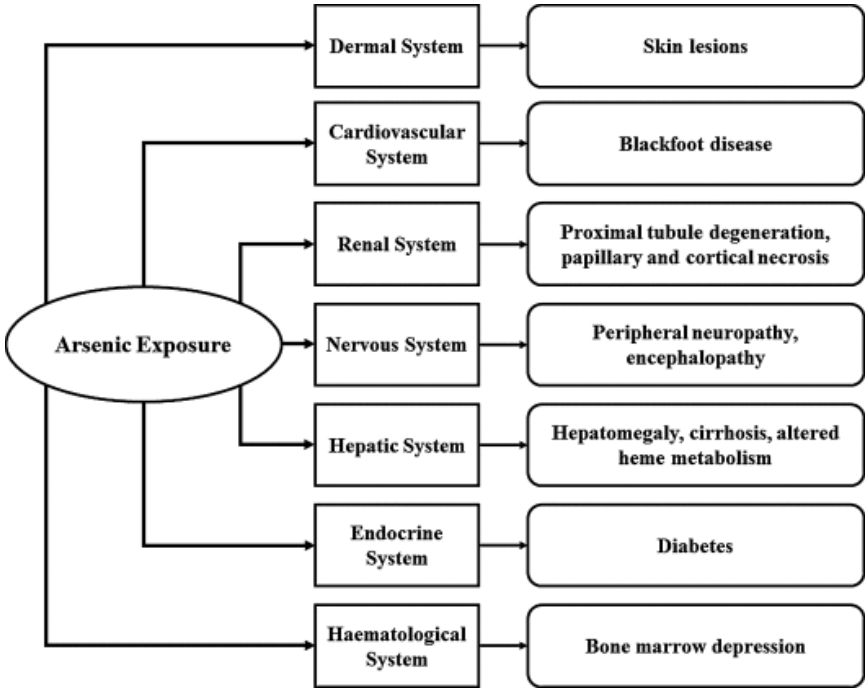


Figure 1.3 Symptoms from As exposure on major organ systems (Abdul 2015)

## 1.3. **Arsenic Standards**

The international standards for As concentration in drinking water were established by the World Health Organization (WHO) since 1958 (WHO 2011). Referring to the WHO guidelines published in 1993 for Drinking Water Quality, the As concentration should be less than 10 µg/L. This guideline was solely based on expansion of As toxicity awareness and its cancerous nature, its technologies to measure its toxicity more accurately. The 2004 standard value in United States is 50 ppb (µg/L). To avoid any permanent effects due to prolonged exposure to As in the drinking water, an updated standard for As presence in water was set to be maintained no more than 10 µg/L, which was made effective since 2006 (US EPA 2001).

## 1.4. **Source of Arsenic**

Arsenic contains in the structure of more than 200 minerals, for example, arsenides, sulfides, and oxides. Table 1.2 shows some of the most common As minerals found in nature and its occurrence (Smedley and Kinniburgh 2002). The majority are ore minerals or their alteration products. These minerals, however, can be hardly found in nature. Arsenic normally exists in direct correction with the transition metal and some other elements such as Cd, Pb, Sb, P, and W. Two most abundont As ore minerals are arsenopyrite (FeAsS) and arsrenian or As-rich pyrite ($Fe(S,As)_2$) (Nordstrom, 2000). Arsenopyrite tends to be the first form of minerals, forming by hydrothermally solution under high temperature (> 100  degree C) before

consecutively changing into rare native As, $Fe(S, As)_2$, realgar (AsS) and orpiment ($As_2S_3$). This can be confirmed by the observation of zonation within sulfide minerals in which FeAsS $Fe(S, As)_2$, and AsS-$As_2S_3$ are sequenced from inner layer (cores) to outer layer (rims), respectively (Smedley and Kinniburgh 2002).

Table 1.2 Major As in nature and its occurrence (Smedley and Kinniburgh 2002)

| **Mineral** | **Occurrence** |
|---|---|
| Native arsenic (As) | Hydrothermal veins |
| Niccolite (NiAs) | Vein deposits and norites |
| Realgar (AsS) | Vein deposits, often associated with orpiment, clays and limestones, also deposits from hot springs |
| Orpiment ($As_2S_3$) | Hydrothermal veins, hot springs, volcanic sublimation products |
| Cobaltite (CoAsS) | High-temperature deposits, metamorphic rocks |
| Arsenopyrite (FeAsS) | The most abundant As mineral, dominantly in mineral veins |
| Tennantite ($(Cu,Fe)_{12}As_4S_{13}$) | Hydrothermal veins |
| Enargite ($Cu_3AsS_4$) | Hydrothermal veins |
| Arsenolite ($As_2O_3$) | Secondary mineral formed by oxidation of arsenopyrite, native arsenic and other As minerals |
| Claudetite ($As_2O_3$) | Secondary mineral formed by oxidation of realgar, arsenopyrite and other As minerals |
| Scorodite ($FeAsO_4.2H_2O$) | Secondary mineral |
| Annabergite ($(Ni,Co)_3(AsO_4)_2.8H_2O$) | Secondary mineral |
| Hoernesite ($Mg_3(AsO_4)_2.8H2O$) | Secondary mineral, smelter wastes |
| Conichalcite ($CaCu(AsO_4)(OH)$) | Secondary mineral |
| Pharmacosiderite ($Fe_3(AsO_4)_2(OH)_3.5H_2O$) | Oxidation product of arsenopyrite and other As minerals |

Arsenic content in common rock-forming minerals is shown in Table 1.3 (Baur, W.H. and Onishi 1969; Boyle and Jonasson 1973; Dudas, 1984; Arehart et al. 1993; Fleet and Mumin, 1997; Pichler et al. 1999; Smedley and Kinniburgh 2002). Chemical properties of As is somewhat similar to sulfur (S). This is why the highest content of As is regularly found in sulfide minerals mostly as a substitution of S in the crystal structure. Apart from sulphide minerals, in many oxide and hydrous metal oxide minerals, As content can also be high. It can be present ether in the mineral structure (i.e., a product of co-precipitation of As with iron oxide/oxy-hydroxide) or as sorbed species (Brannon and Patrick 1987; Hiemstra and van Riemsdijk 1996). Arsenic content in some phosphate minerals such as apatite can reach up to 1000 mg/kg. However, the phosphate minerals have a small contribution to the As content in most of the cases due to less availability of phosphate minerals in nature compared with sulfide, oxide, and hydrous metal oxide minerals. Low level of As can be observed in the other common rock-forming minerals such as silicate and carbonate minerals.

Arsenic is naturally found only in trace amounts in rocks. However, it can be concentrated in certain types of rocks, such as hydrothermally altered rocks. Hydrothermally altered rocks refer to rocks that have undergone an alteration by geothermal fluids, causing them to commonly contain As-bearing minerals (Pirajno 2009). Exposure of these types of rocks to oxygen ($O_2$) and water leads to a potential source of As contamination of soil and groundwater.

According to the geological conditions in Hokkaido, Japan, considerable amounts of rocks have undergone hydrothermal alterations, causing them to contain elevated amounts of As (Fig. 1.4) (AIST, 2017). Thus, the ongoing tunnel construction projects in this region, e.g., the rout expansion project of Hokkaido Shingansen (Fig. 1.5) (Hokkaido Shinkansen 2017), lead to a production of a massive amount of hydrothermally altered rock. Improper disposal of these excavated rocks will present a problem, which poses a potential environmental hazard, particularly to soil and groundwater.

Table 1.3 rsenic content in common rock-forming minerals (Smedley and Kinniburgh 2002)

| **Mineral** | **As content range (mg kg$^{-1}$)** |
|---|---|
| ***Sulfide minerals:*** | |
| Pyrite | 100–77,000 |
| Pyrrhotite | 5–100 |
| Marcasite | 20–126,000 |
| Galena | 5–10,000 |
| Sphalerite | 5–17,000 |
| Chalcopyrite | 10–5000 |
| ***Oxide minerals:*** | |
| Hematite | <160 |
| Fe oxide (undifferentiated) | <2000 |
| Fe(III) oxyhydroxide | <76,000 |
| Magnetite | 2.7–41 |
| Ilmenite | <1 |
| ***Silicate minerals:*** | |
| Quartz | 0.4–1.3 |
| Feldspar | <0.1–2.1 |
| Biotite | 1.4 |
| Amphibole | 1.1–2.3 |
| Olivine | 0.08–0.17 |
| Pyroxene | 0.05–0.8 |
| ***Carbonate minerals:*** | |
| Calcite | 1–8 |
| Dolomite | <3 |
| Siderite | <3 |
| ***Sulfate minerals:*** | |
| Gypsum/anhydrite | <1–6 |
| Barite | <1–12 |
| Jarosite | 34–1000 |
| ***Other minerals:*** | |
| Apatite | <1–1000 |
| Halite | <3–30 |
| Fluorite | <2 |

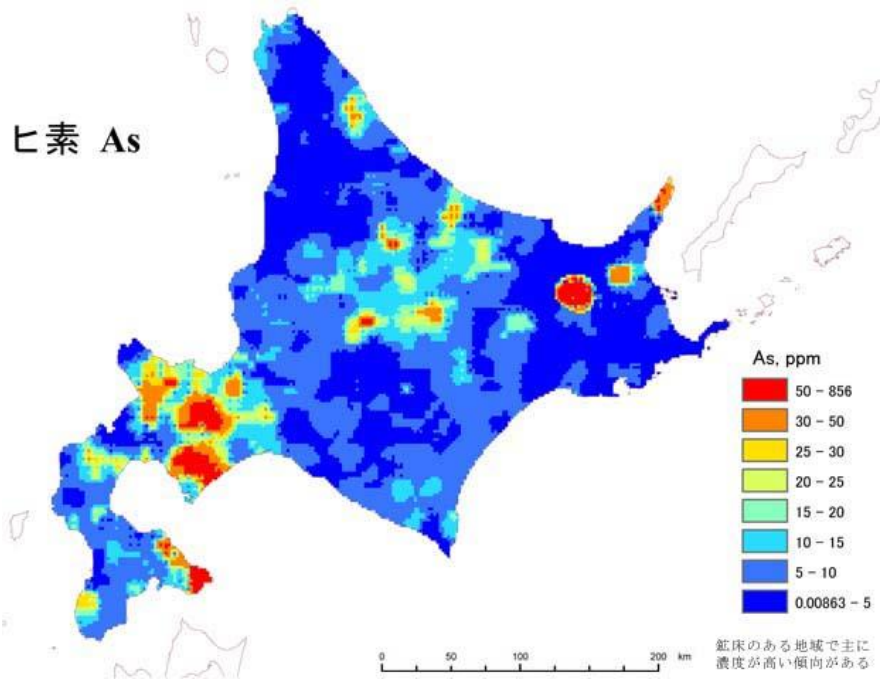


Figure 1.4 Arsenic distribution in Hokkaido
(https://gbank.gsj.jp/geochemmap/Hokkaido/gazou/hokkaidoAs-s.jpg)


Figure 1.5 Rote of Hokkaido Shinkansen
(https://ja.wikipedia.org/wiki/北海道新幹線)

## 1.5. **The Method of Arsenic Removal**

The removal of inorganic As from water can be done by many treatment technologies. Conventional coagulation and filtration process are often used in large-scale water treatment facilities to remove As contamination from water by precipitation with alum or iron salts, which are the two most common coagulants used in water treatment industry (Lakherwal 2014). In addition, lime softening process is another potential method to remove As from water. On the other hand, different approaches and methods such as anion exchange resins, reverse osmosis or adsorption are used for As removal in smaller scale water treatment facilities and point of entry system (Cartwright 1985; Clifford 1990; Kwon et al. 2010).

Among these methods, adsorption is the proper treatment technique for blocking or retarding the leaching of As from the excavated hydrothermally altered rock due mainly to its simplicity and cost effectiveness (Yadanaparthi et al. 2009).

## 1.6. **Adsorption Theory**

Adsorption is different from absorption. Adsorption is the adhesion of the substance (adsorbate) onto the surface of the adsorptive material (adsorbent). While absorption is the passage of the substance into the bulk of the medium. There are two classifications of adsorption; chemical adsorption and physical adsorption. However, there is no acute distinction to distinguish between the two interactions. Chemical adsorption or chemisorption involves a chemical reaction in which the forming of strong, valence bonds between adsorbate molecules and adsorbent surface, known as active sites, occurs. It occupies certain active sites on the surface and the activation energy is needed. Only monolayer of chemisorbed molecules is formed and the process is irreversible. Therefore, chemisorption is generally used to evaluate the number of surface active sites. On the other hand, physical adsorption (physisorption) is adsorption in which it involves weaker interaction, intermolecular forces or so called Van der Waals and electrostatic forces. There is no compound formation in physisorption. The process is reversible and does not require any activation energy. Moreover, multilayer of adsorbate can be formed (Adamson 1990).

There are many factors affecting adsorption, such as adsorbent surface properties and polarity, nature and concentration of the adsorbate, the temperature and pH of the solution and the presence of competing solutes. The properties of adsorbent surface, such as surface area and pore size are very significant in the adsorption process. Absorbents are classified based on their porosity, as porous or nonporous adsorbents. Nonporous adsorbents provide relatively small external adsorptive surface areas, while porous adsorbents provide large internal adsorptive surface areas. For nonporous adsorbents, such as glass, steel beads and clay, the

maximum amount of adsorption is proportional to the amount of surface area of the adsorbent that adsorbate can access. On the other hand, for porous adsorbate that has significantly larger surface area, however, the surface area of porous adsorbent does not have a significant influence on adsorption capacity (Toth 2001; Dabrowsk 2001).

Steric, equilibrium, and kinetic mechanisms are three processes controlling the characteristics of adsorption (Do 1998). The steric mechanism is one of the mechanisms controlling thermodynamic properties of adsorption, especially in term of the heat of adsorption. The amount heat emitted from the adsorption is known as iso-steric heat. However, in liquid-phase adsorption system, adsorption of solute molecules and desorption of water molecules usually occur simultaneously, resulting in the low amount of steric heat in such a case. Therefore, equilibria isotherm and kinetic mechanism are two main parameters used to characterize the liquid-phase adsorption system.

### 1.6.1. **Adsorption kinetic**

Kinetic of adsorption indicates the solute uptake rate. It is important factor in designing the water treatment process. Recently, considerable amounts of adsorption kinetic models have been developed to describe the mechanisms of adsorption process (Qiu et al. 2009). These mathematical models can be classified into two groups according to the basis of the derivation. Adsorption diffusion models were developed considering the three following steps: first, the diffusion of adsorbent across the stationary liquid film covering the solid particle, next, the diffusion inside the pores space (internal or intra-particle diffusion), and finally, the attachment and detachment between the adsorbate and active sites (i.e., mass action) (Lazaridis and Asouhidou 2003). Adsorption reaction models are derived based on chemical reaction kinetic equations, meaning that the kinetics are analyzed regardless of the steps mentioned above. Unfortunately, the velocity of liquid infiltrating through the adsorption layer in this study is generally very slow. Therefore, the study of kinetic adsorption model can be ignored.

### 1.6.2. **Adsorption equilibria**

Similar to the equilibrium concept of the chemical reaction, if the contact time of the adsorbent and adsorbate is long enough, the system will reach equilibrium. The equilibrium behaviors can be reported in term of adsorption isotherm.

Adsorption isotherm is a curve describing a relationship between the amounts of substance adsorbed on the solid surface ($q_e$) and remaining in the solution ($c_e$) at constant

temperature and pH. Many different models of adsorption isotherms have been proposed in which the individual isotherm indicates different ways of how adsorbents interact with the solid materials (Foo and Hameed 2010). The properties of adsorbate are key parameters, determining a suitable model. Linear, Langmuir, and Feundlich isotherms are three common models, used for predicting the equilibrium behavior in liquid phase due to its simplicity. Each model was derived from difference assumption. The shapes of each isotherms are shown in Fig. 1.6.

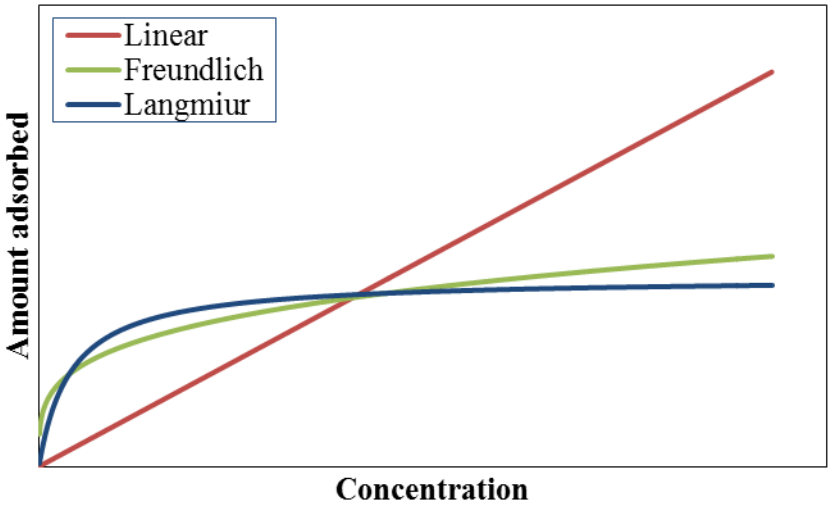


Figure 1.6 Shapes of Linear, Langmuir, and Freundlich isotherms

**Linear isotherm**: The main assumptions of linear adsorption isotherm are; first, the solid surface has infinite number of open-sites (this is only true when the concentration of solute is very low) and second, the adsorbate is homogeneous, therefore, each adsorbed molecule generates constant enthalpies and activation energy (Erbil 2006; Limousin et al. 2007). The Linear adsorption isotherm can be calculated using equation given below:

$$q_e = K_D \times C_e \qquad (1.1)$$

where $q_e$, $C_e$, and $K_D$ is the amount of adsorbed adsorbate per unit mass of adsorbent (mg/g), the concentration of adsorbent in the solution at equilibrium condition (mg/L), and the distribution confident (L/g), respectively.

**Langmuir isotherm**: The only difference assumption between the linear and Langmuir adsorption isotherm is that in Langmuir adsorption isotherm, the adsorption can only occur on a limited number of open-sites (the adsorption can occur to some certain extend) (Vijayaraghavan et al. 2006; Kundu and Gupta 2006). The mathematical equation can be expressed as follow:

$$q_e = \frac{q_m b C_e}{1 + b C_e} \quad (1.2)$$

Or

$$\frac{C_e}{q_e} = \frac{1}{q_m} C_e + \frac{1}{q_m b} \quad (1.3)$$

where $q_m$ is the maximum adsorption capacity of the solid (mg/g) and $b$ is the affinity of the adsorbent for the solute of interest.

**Freundlich isotherm**: This type of isotherm is an empirical model. It can be able to use to describe the non-ideal adsorption according to the assumption of multilayer adsorption and heterogeneous surface (Adamson and Gast 1997). However, Freundlich adsorption isotherm is applicable for both the monolayer (chemisorption) and multilayer adsorptions.

$$q_e = K_F \times C_e^{1/n} \quad (1.4)$$

Or

$$\log q_e = \log K_F \times \frac{1}{n} \log C_e \quad (1.5)$$

Where $K_F$ and *n* correspond to the empirical constants. If "$1/n$" is in between "0" and "1", this value indicates the intensity of surface heterogeneity. The lower the value, the more heterogeneous the surface becomes. In contrast, a value above "1" implies monolayer process whereas the value of "$1/n$" indicates a cooperative adsorption (Haghseresht and Lu 1998).

## 1.7. Modeling of Reactive Solute Transport in Unsaturated Porous Media

The behavior of contaminant migration is governed by many factors, including physical, chemical, and biological processes of the media, characteristics of water flow, and characteristics of contaminant itself (Robinson and Lucas 1985; Jensen and Christensen 1999; Oygard et al. 2004; Rapti-Caputo and Vaccaro 2006). Therefore, modeling is an appropriate technique for helping us to understand the movement of contaminants and to design a system to prevent the leaching of hazardous chemicals from such application as landfills. This has led to the development of a variety of analytical and numerical models to simulate and predict the transport of hazardous chemicals in a variably saturated zone in the past few decades. The most

popular models used to predict the solute transport and water movement in variably saturated zones are advection-dispersion equation and Richards equation, respectively (Simunek et al. 2008). The advection-dispersion equation (Equation 1.6) is derived from a simple mass balance equation. The mathematical expression for one dimensional advection-dispersion in saturated media is shown below:

$$\frac{\partial \theta c}{\partial t} = \frac{\partial}{\partial z}\left[\theta D \frac{\partial c}{\partial z}\right] - \frac{\partial qc}{\partial z} - \rho \frac{\partial s}{\partial t} - Q \qquad (1.6)$$

where, $\theta$ is the volumetric water content ($cm^3/cm^3$), $c$ is the solution concentration ($mmol/cm^3$), $t$ is time (h), $z$ is the vertical axis (cm), $D$ is the hydrodynamic dispersion coefficient ($cm^2/h$), $\rho$ is the bulk density ($g/cm^3$), $s$ is the amount of solute adsorbed on soil matrix (mmol/kg of adsorbent), and $Q$ is the sink for irreversible solute interaction, sorption, and degradation terms ($mmol/h*cm^3$). The hydrodynamic dispersion coefficient ($cm^2/h$) ($D$) is given by:

$$D = \propto q \qquad (1.7)$$

and Darcy soil water flow velocity (cm/h) ($q$) by:

$$q = -K\left(\frac{\partial H}{\partial z}\right) \qquad (1.8)$$

where $\propto$ is the dynamic dispersivity (cm), $K$ is the saturated hydraulic conductivity (cm/h), and $H$ is the hydraulic head.

In unsaturated zone, the water movement is calculated by using the following equations:

$$\frac{\partial \theta}{\partial t} = \vec{\nabla} \cdot \left(\sum_{i=1}^{n} \overrightarrow{q_{i,in}} - \sum_{j=1}^{m} \overrightarrow{q_{J,out}}\right) \qquad (1.9)$$

Put Equation (1.9) in one-dimensional (1D) form in the direction of $z$:

$$\frac{\partial \theta}{\partial t} = \frac{\partial}{\partial z} q \qquad (1.10)$$

Darcy soil water flow velocity in unsaturated medium is given by:

$$q = -K(\theta)\left(\frac{\partial H}{\partial z}\right) \qquad (1.11)$$

and $H$ is defined as:

$$H = h - z \tag{1.12}$$

where $K(\theta)$ is the unsaturated hydraulic conductivity (cm/h) and $h$ is the matrix head (cm). Substituting $H$ into Equation (1.11) and $q$ into Equation (1.10), we finally get:

$$\frac{\partial \theta}{\partial t} = \frac{\partial}{\partial z}[K(\theta)\left(\frac{\partial h}{\partial z} + 1\right)] \tag{1.13}$$

Equation (1.13) is known as Richards equation, which is derived from a mass balance equation together with unsaturated Darcy equation in $z$ direction.

Several empirical models have been developed for estimating $K(\theta)$ (eg., Jackson 1972; Kunze et al. 1968; Millington and Quirk 1961; Mualem 1976;Toledo et al. 1990; van Genuchten 1980). van-Genuchten relationship is known to be the model that can be used to estimate $K(\theta)$ for most of soil textures (van-Genuchten et al. 1991). The van-Genuchten equations are as follow:

$$K(\theta) = K_s {S_e}^{l}[1 - (1 - S_e^{\frac{1}{m}})^m]^2 \tag{1.14}$$

$$\theta(h) = \theta_r + \frac{\theta_s - \theta_r}{[1+|\alpha h|^n]^m} \tag{1.15}$$

$$m = 1 - \frac{1}{n}, n > 1 \tag{1.16}$$

where $\theta_s$ is the saturated water content ($cm^3/cm^3$), $\theta_r$ is the residual water content ($cm^3/cm^3$), $K_s$ is the saturated hydraulic conductivity, and $\alpha$ and $n$ are fitted parameters determining the shape of the soil water retention curve. The effective saturation ($S_e$) is determined by:

$$S_e = \frac{\theta - \theta_r}{\theta_s - \theta_r} \tag{1.17}$$

Therefore, the reactive solute transport in both saturated and unsaturated media can be simulated by the combination of Equations (1.6) and (1.13).

A large number of researchers have studied on solving an analytical solution for reactive solute transport in variably saturated media (Cho 1971; Wagenet et al. 1976; Higashi

and Pigford 1980; van-Genuchten 1985). However, the solutions for such complicated conditions as solute transport with unsteady water flow and non-equilibrium transport of solute involving in nonlinear reactions, still cannot be derived. Thus, numerical models must be applied. Many computer programs have been developed to simulate the complex situations of solute transport. Hydrus-1D is one of the computer codes capable of numerically solving the governing equations for solute transport in unsaturated, partially saturated, and fully saturated porous media (Simunek et al. 2008). It is proved by many studies about its capability of simulating a simple solute transport in complex soil water regime (Ma et al. 2010; Wang et al. 2010; Tafteh and Sepaskhah 2012; Ogden et al. 2015). The code is written based on Galerkin Liner Finite Element method (Simunek et al. 2008). In this study, Hydrus-1D was applied to simulate a As transport through an unsaturated adsorption layer.

## 1.8. **Problem Statement and Objectives of the Study**

Hydrothermally altered rocks are frequently encountered when tunnels are constructed in Hokkaido, Japan. High concentrations of hazardous elements, such as As, are often released from these rocks into the surrounding environments. A massive amount of hydrothermally altered rocks is expected to be produced from the ongoing tunnel construction projects. Improper disposal of these excavated rocks will present a problem, which poses a potential environmental hazard, particularly to soil and groundwater. At present, the excavated rocks are regularly disposed to specially designed landfills to minimize the contact of the rocks with surrounding environments (Katsumi et al. 2001). These methods of disposing, however, are economically infeasible. Thus, factors controlling the mobility of As from hydrothermally altered rocks are needed to be investigated to develop a reasonable technique for disposing of these waste rocks. Recently, several studies have investigated the mechanisms of As migration from hydrothermally altered rocks by using laboratory column experiments. This study aims to expand those previous results by focusing on two concerns: (1) developing a method to demonstrate the effects of water content and oxygen ($O_2$) concentration in relation to adding covering and adsorption layers on As leaching by introducing water content and oxygen concentration sensors into columns, and (2) modeling of As migration to provide insights into the transport phenomena of As through an adsorption layer by using Hydrus-1D.

## 1.9. Research Layout

This dissertation contains 5 chapters.

Chapter 1 illustrates a literature review on basic knowledges about As including general properties, effects on human health, sources specifically in rock-forming minerals, common technics to remove aqueous As. This chapter also includes the basic adsorption theories. At the end of the chapter, modeling of solute migration in vadose zones is introduced.

Chapter 2 describes the relationships of water content and $O_2$ concentration on As leaching behaviors in relation to additional layer(s) in laboratory column experiments. Two water content and one oxygen concentration sensors were introduced into every column, and the monitoring was done over a period of 30 weeks. The experimental setup and procedures used in this study were explained in detail. The full results and discussion on the properties of solid samples, effects of additional layer(s) on water content and oxygen concentration, effects of additional layer(s) on pH, oxidation-reduction potential, electrical conductivity, and coexisting ions, and effects of additional layer(s) on As release were also summarized in this section.

Chapters 3 and 4 present the reactive transport modeling of As through an unsaturated adsorption layer by using Hydrus-1D. The model parameters, initial and boundary conditions, and assumptions were reported. Chapter 3 presents results and discussion on the simulation of water movement in unsaturated media to confirm the ability of Hydrus-1D to simulate the reactive transport of As. On the other hand, in chapter 4, the mechanisms of As movement based on experimental and simulation results were discussed.

Finally, general conclusion and recommended method for disposing the waste rock were made in the last chapter.

## References


Abdul, K. S. M., Jayasinghe, S. S. E., Chandana, P.S., Jayasumana, C., De Silva, P. M. C. S. (2015). Arsenic and human health effects: A review, Environmental Toxicology and Pharmacology. 40(3), 828-846.

Adamson, A. W. (1990). Physical Chemistry of Surfaces, Wiley, New York.

Adamson, A. W., Gast, A. P. (1997). Physical Chemistry of Surfaces (sixth ed.). Wiley-Interscience. New York.

AIST (National Institute of Advanced Industrial Science and Technology), (2017). Geological survey, https://gbank.gsj.jp/geochemmap/Hokkaido/gazou/hokkaidoAs-s.jpg, last visited June 2017.

Arehart, G. B., Chryssoulis, S. L., Kesler, S. E. (1993). Gold and arsenic in iron sulfides from sediment-hosted disseminated gold deposits: Implications for depositional processes. Economic Geology, 88, 171–185.

Baur, W. H., Onishi, B. M. H. (1969). Arsenic. K. H. Wedepohl (Ed.). Handbook of Geochemistry, Springer-Verlag.

Brannon, J. M., Patrick, W. H. (1987). Fixation, transformation, and mobilization of arsenic in sediments. Environmental Science and Technology, 21, 450–459.

Brookins, D. G. (1988). Eh-pH diagrams for geochemistry. Springer-Verlag, Berlin.

Boyle, R. W., Jonasson, I. R. (1973). The geochemistry of As and its use as an indicator element in geochemical prospecting. Journal of Geochemical Exploration, 2, 251–296.

Buchanan, W. D., 1962. Toxicity of arsenic compounds. Elsevier Publishing Company, New York, USA.

Cartwright, P. S., (1985). Membranes separations technology for industrial effluent treatment - A review. Desalination, 56, 17-35.

Cho, C. M., (1971). Convective transport of ammonium with nitrification in soil. Canadian Journal of Soil Science, 51(3), 339-350.

Chu, H. A., Crawford-Brown, D. J. (2006). Inorganic arsenic in drinking water and bladder cancer: a meta-analysis for dose-response assessment. Int. J. Environ. Res. Public Health, 3 (4), 316–22.

Clifford, D. A. (1990). Ion exchange and inorganic adsorption. AWWA, Water Quality and Treatment, 4th edition. McGraw-Hill, New York.

Cross, J. D., Dale, I. M., Leslie, A. C. D., Smith, H. (1979). Industrial exposure to arsenic. Journal of Radioanalytical Chemistry, 48, 197–208.

Dabrowsk, A. (2001). Adsorption-from theory to practice. Advances in Colloid and Interface Science, 93, 135-224.

Do, D. D. (1998). Adsorption Analysis: Equilibria and Kinetics. Imperial College Press, London.

Dudas, M. J. (1984). Enriched levels of arsenic in post-active acid sulfate soils in Alberta. Soil Science Society of America Lournal, 48, 1451–1452.

Environmental Protection Agency (EPA) U.S.A. (1993). Mercury and arsenic wastes: Removal, recovery, treatment, and disposal. Park Ridge, N.J., U.S.A.: Noyes Data Corporation.

Erbil, H. Y. (2006). Surface Chemistry of Solid and Liquid Interfaces. Wiley-Interscience. New York.

Ferguson, J. F., Gavis, J., 1972. Review of the arsenic cycle in natural waters. Water Research, 6, 1259-1274.

Fleet, M. E., Mumin, A. H. (1997). Gold-bearing arsenian pyrite and marcasite and arsenopyrite from carlin trend gold deposits and laboratory synthesis. American Mineralogist, 82, 182–193.

Foo, K. Y., Hameed, B. H. (2010). Insights into the modeling of adsorption isotherm systems. Chemical Engineering Journal, 156(1), 2-10.

Ghimire, K. N., Inoue, K., Yamaguchi, H., Makino, K., Miyajima, T. (2003). Adsorptive separation of arsenate and arsenite anions from aqueous medium by using orange waste. Water Research, 37(20), 4945-4953.

Glazener, F. S., Ellis, J. G., Johnson, P. K. (1968). Electrocardiographic findings with arsenic poisoning. Calif. Med.,109, 158-162,

Haghseresht, F., Lu, G. (1998). Adsorption characteristics of phenolic compounds onto coal-reject-derived adsorbents. Energy Fuels, 12, 1100–1107.

Higashi, K., Pigford, T. H. (1980). Analytical models for migration of radionuclides in geologic sorbing media. Journal of Nuclear Science and Technology, 7(9), 700-709.

Hiemstra, T., van Riemsdijk, W. H. (1996). A surface structural approach to ion adsorption: the charge distribution, CD. Model. Journel of Colloid Interface Science, 179, 488–508.

Hokkaido Shinkansen. (2017). https://ja.wikipedia.org/wiki/北海道新幹線, last visited June 2017.

Hong, Y. S., Song, K. H., Chung, J.Y. (2014). Health effects of chronic arsenic exposure. Journal of Preventive Medicine and Public Health, 47(5), 245-52.

Jackson, R. D. (1972). On the calculation of hydraulic conductivity. Soil Science Society of America Journal, 36, 380-382.

Katsumi, T., Benson, C. H., Foose, G. J., Kamon, M. (2001). Performance-based design of landfill liners. Engineering Geology, 60(1-4). 139-148.

Kingston, R. L., Hall, S., Sioris, L. (1993). Clinical observations and medical outcome in 149 cases of arsenate ant killer ingestion. J. Toxicol. Clin. Toxicol., 31 (4), 581–91.

Kundu, S., Gupta, A. K., (2006). Arsenic adsorption onto iron oxide-coated cement (IOCC): Regression analysis of equilibrium data with several isotherm models and their optimization. Chemical Engineering Journal, 122, 93–106.

Kunze, R. J., Uehara, G., Graham, K. (1968). Factors important in the calculation of hydraulic conductivity. Soil Science Society of America Journal, 32, 760-765.

Kwon, J. S., Yun, S. T., Lee, J. H., Kim, S. O., Jo, H. Y. (2010), Removal of divalent heavy metals (Cd, Cu, Pb, and Zn) and arsenic (III) from aqueous solutions using scoria: Kinetics and equilibrium of sorption, Journal of Hazard Mater, 174, 307–313.

Lakherwal, D. (2014). Adsorption of heavy metals: A review. International Journal of Environmental Research and Development, 4(1), 41-48.

Lazaridis, N. K., Asouhidou, D. D. (2003). Kinetics of sorptive removal of chromium(VI) from aqueous solutions by calcined Mg-Al-$CO_3$ hydrotalcite. Water Research, 37(12), 2875-2882.

Limousin, G., Gaudet, J. P., Charlet, L., Szenknect, S., Barthes, V., Krimissa, M. (2007). Sorption isotherms: A review on physical bases, modeling and measurement. Applied Geochemistry, 22, 249-275.

Ma, Y., Feng, S., Su, D., Gao, G., Huo, Z. (2010). Modeling water infiltration in a large layered soil column with a modified Green–Ampt model and HYDRUS-1D. Computers and Electronics in Agriculture, 71, S40-S47.

Matschullat, J. (2000). Arsenic in the geosphere: A review. The Science of the Total Environment, 249 (1–3), 297–312.

Millington, R. J., Quirk, J. P. (1961). Permeability of porous solids. Transactions of the Faraday Society, 57, 1200-1207.

Mualem, Y. (1976). A new model for predicting the hydraulic conductivity of unsaturated porous media. Water Resources Research, 12, 513-522.

Murphy, E. A., Aucott, M. (1998). An assessment of the amounts of arsenical pesticides used historically in a geographical area. Science of the Total Environment, 218 (2–3), 89–101.

Nordstrom, D. K. (2000). An overview of arsenic mass poisoning in Bangladesh and West Bengal, India. Society for Mining, Metallurgy and Exploration, 21–30.

Penrose, W. R. (1974). Arsenic in the marine and aquatic environments; Analysis, occurrence and significance. CRC Critical Reviews in Environmental Control, 4, 465-482.

Pichler, T., Veizer, J., Hall, G. E. M. (1999). Natural input of arsenic into a coral reef ecosystem by hydrothermal fluids and its removal by Fe(III) oxy-hydroxides. Environmental Science and Technology, 33, 1373–1378.

Pirajno, F., (2009). Hydrothermal Processes and Mineral Systems. The Natherlands, Springer Science.

Ogden, F. L., Lai, W., Steinke, R. C., Zhu, J., Talbot, C. A., Wilson, J. L. (2015). A new general 1-D vadose zone flow solution method. Water Resources Research, 51(6), 4282-4300.

Oygard, J. K., Mage, A., Gjengedal, E. (2004). Estimation of the mass balance of selected metals in four sanitary landfills in Western Norway, with emphasis on the heavy metals content of the deposited waste and the leachate. Water Research, 38(12), 2851-2858.

Qiu, H., Lv, L., Pan, B. C., Zhang, Q. J., Zhang, W. M., Zhang, Q. X. (2009). Critical review in adsorption kinetic models. Journal of Zhejiang University Science A, 10(5), 716-724.

Rahman, F. A., Allan, D. L., Rosen, C. J., Sadowsky, M. J. (2004). Arsenic availability from chromated copper arsenate (CCA)-treated wood. Journal of Environmental Quality, 33 (1), 173–80.

Rapti-Caputo, D. Vaccaro, C. (2006). Geochemical evidences of landfill leachate in groundwater. Engineering Geology, 85, 111-121.

Robinson, H. D., Lucas J. L. (1985). Leachate attenuation in the unsaturated zone beneath landfills: Instrumentation and monitoring of a site in southern England. Water Science and Technology, 17, 477-492.

Rose, M., Lewis, J., Langford, N., Baxter, M., Origgi, S., Barber, M., MacBain, H., Thomas, K. (2007). Arsenic in seaweed—Forms, concentration and dietary exposure. Food and Chemical Toxicology, 45(7), 1263-1267.

Simunek, J., van Genuchten, M. T., Sejna, M. (2008). Development and applications of the HYDRUS and STANMOD software packages and related codes. Vadose Zone, 7(2), 587-600.
Smedley, P. L., Kinniburgh, D. G. (2002). A review of the source, behavior and distribution of arsenic in natural waters. Applied Geochemistry, 17(5), 517-568.

Tafteh, A., Sepaskhah, A. R. (2012). Application of HYDRUS-1D model for simulating water and nitrate leaching from continuous and alternate furrow irrigated rapeseed and maize fields. Agricultural Water Management, 113, 19-29.

Thomas, D. J., Bradham, K. (2016). Role of complex organic arsenicals in food in aggregate exposure to arsenic. Journal of Environmental Sciences, 49, 86-96.

Toledo, P. G., Novy, R. A., Davis, H. T., Scriven, L. E. (1990). Hydraulic conductivity of porous media at low water content, Soil Science Society of America Journal. 54, 673-679.

Toth, J. (2001). Adsorption: Theory, Modeling, and Analysis. Marcel Dakker, New York.

US EPA (2001). Arsenic rule benefits analysis: An SAB review. [EPA-SAB-RSAC-01 -005].

van Genuchten, M. T. (1980). A closed-form equation for predicting the hydraulic conductivity of unsaturated soils. Soil Science Society of America Journal, 44, 892–898.

van Genuchten, M. T. (1985). Convective-dispersive transport of solutes involved in sequential first-order decay reactions. Computers & Geosciences, 11(2), 129-147.

Jensen, D. L., Christensen, T. H. (1999). Colloidal and dissolved metals in leachate from four Danish landfills. Water Research, 33(9), 2139-2147.

van Genuchten, M. T., Leij, F. J., Yates, S. R. (1991). The RETC code for quantifying the hydraulic functions of unsaturated soils. USEPA Report 600/2-91/065. U.S. Environmental Protection Agency, Ada, Oklahoma.

Vijayaraghavan, K., Padmesh, T. V. N., Palanivelu, K., Velan, M. (2006). Biosorption of nickel(II) ions onto Sargassum wightii: Application of two-parameter and three parameter isotherm models. Journal of Hazardous Material, 133, 304–308.

Wagenet, R. J., Biggar, J. W., Nielsen, D. R. (1976). Analytical solutions of miscible displacement equations describing the sequential microbiological transformations of urea, ammonium and nitrate, Research Report no 6001, Department of Water Science and Engineering, University of California, Davis, CA.

Wang, H., Ju, X., Wei, Y., Li, B., Zhao, L., Hu, K. (2010). Simulation of bromide and nitrate leaching under heavy rainfall and high-intensity irrigation rates in North China Plain. Agricultural Water Management, 97, 1646–1654.

WHO (World Health Organization) (2011). Guidelines for drinking-water quality. 4th edition.

Yan, X. P., Kerrich, R., Hendry, M. J. (2000). Distribution of arsenic(III), arsenic(V) and total inorganic arsenic in porewaters from a thick till and clay-rich aquitard sequence, Saskatchewan, Canada. Geochim. Cosmochim. Acta, 64, 2637–2648.

Yadanaparthi, S. K. R., Graybill, D. and Wandruszka, R. (2009). Adsorbents for the removal of arsenic, cadmium, and lead from contaminated waters. Journal of Hazardous Material, 171, 1-15.

# Chapter 2

# EFFECTS OF ADDITIONAL LAYER(S) ON MOBILITY OF ARSENIC FROM HYDERTHRMALLY ALTERED ROCK IN LABORATORLY COLUMN EXPERIMENTS

## 2.1. Introduction

In Hokkaido, Japan, rocks excavated by tunnel construction usually contain hydrothermally altered rocks (Takahashi et al. 2011; Tabelin et al. 2012a). Thus, as a result of improper disposal, leachates containing high concentrations of As are generated and may contaminate the surrounding environment, in particular groundwater and soil. Currently, the excavated rocks are often disposed in specially designed landfills (Katsumi et al. 2001). However, they are economically infeasible. Therefore, investigation into the factors controlling the mobility of As is required to design alternative disposal techniques of these potentially hazardous waste rocks.

The mobility of As from hydrothermally altered rocks is generally governed by precipitation, dissolution, adsorption, and desorption reactions, which are highly pH- and redox-dependent (Appelo and Postma 2005; Foster et al. 1998; Savage et al. 2000; Tabelin and Igarashi 2009). In our previous studies, we have reported the parameters controlling the mobility of As from hydrothermally altered rocks by using laboratory column experiments to mimic the actual disposal (Tabelin et al. 2012a, b, 2014). However, the relationship between the conditions of the columns, such as oxygen ($O_2$) concentration and water content, and As leaching was not well described by those experimental setups. These two parameters may act as the fundamental key components of As release (Tabelin and Igarashi 2009; Tabelin et al. 2012a). Therefore, a more in-depth understanding of the mechanisms is still needed since it can be applied to the development of countermeasures that can be used to minimize the mobility of As from hazardous waste rocks. Herein, we have developed a method to demonstrate the effects of water content and $O_2$ concentration in relation to adding covering and adsorption layers on As leaching by introducing water content and $O_2$ concentration sensors into columns. By using the laboratory columns, $O_2$ concentration and water content were continuously monitored while simulated rain was irrigated. This chapter will allow a better understanding of As migration mechanisms from the rocks together with the development of disposal techniques for hazardous waste rocks.

## 2.2. Materials and Methods

### 2.2.1. Sample collection and preparation

The rock sample used in this study was collected from an interim storage site of a tunnel construction in Nakakoshi, Hokkaido, Japan. The rock had been stored in impoundment for about 6 months before sampling to determine the final disposal because the hydrothermally altered rock contained As. The bulk-excavated rock sample was taken by shovels at random points. The particle size ranged from about 20 cm (large particle) to <2 mm (fine particle) in diameter, and the bulk-excavated rock refers to the mixture of altered and unaltered rocks. In practice, during excavation, transportation, interim impoundment, and final disposal, the excavated rock can be naturally crushed into smaller particles. Therefore, in preparation, the rock was air-dried under ambient conditions, crushed by a jaw crusher, sieved with a 2-mm aperture screen, and completely mixed to have a similar distribution of the particle size in columns to conservatively evaluate the risk. Finally, the sample was kept in air-tight containers to minimize oxidation.

Two natural geologic materials, river sediment and volcanic ash, were used as covering and adsorption layers. The river sediment was taken from a river located near the waste rock storage site while the volcanic ash came from the central part of Hokkaido. Sampling was also done by using shovels at random points. The same preparation process as the waste rock sample was also applied to these natural geologic materials.

### 2.2.2. Solid sample characterization

Pressed samples of finely crushed powder (<50 μm in diameter) of the rock and natural geologic materials were prepared for chemical and mineralogical analysis by X-ray fluorescence spectrometer (XRF) (Spectro Xepos, Rigaku Corporation, Japan) and X-ray diffractometer (XRD) (MultiFlex, Rigaku Corporation, Japan). The organic carbon (OC) content was obtained using the total carbon (TC) content and inorganic carbon (IC) content. The TC and IC were analyzed using a total carbon analyzer together with a solid sample combustion unit (TOC-VCSH-SSM-5000A, Shimadzu Corporation, Japan). The surface charges of the river sediment and volcanic ash were measured using Nano-ZS-60 (Malvern Instruments, UK), and the pH was adjusted by 0.1 M hydrochloric acid (HCl) or 0.1 M sodium hydroxide (NaOH).

### 2.2.3. **Column experiments**

#### 2.2.3.1.**Apparatus**

Figure 2.1 illustrates the laboratory column setup and dimensions of the columns. These columns were placed under ambient conditions to mimic the actual disposal environment. The columns, rainfall simulators, and stand were made of transparent polyvinyl chloride. All the columns were vertically mounted on the top of the stand and covered with the rainfall simulator. The covers were designed to have small holes for simulating actual rainfall and to protect the surface of the column from dust.

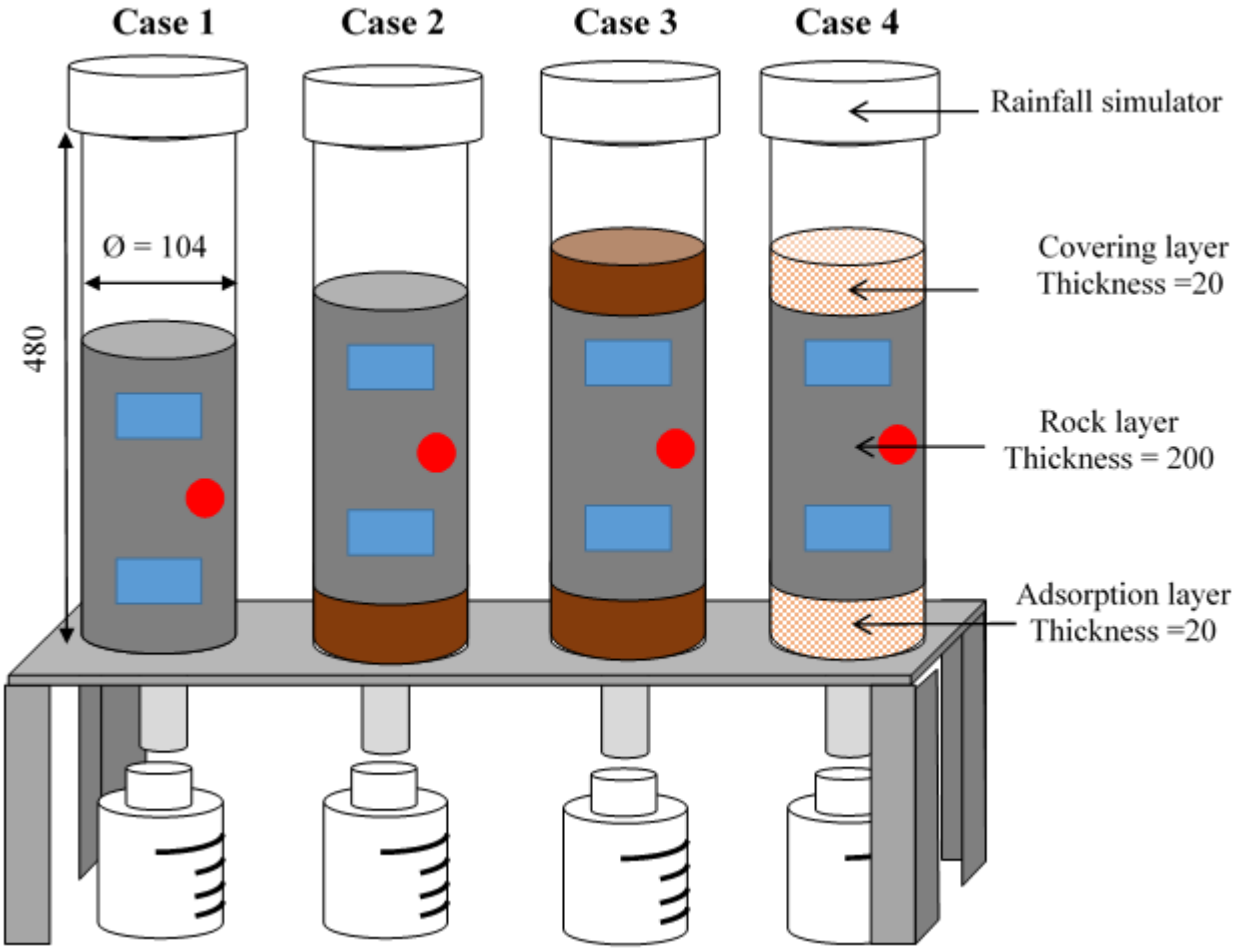


Figure 2.1 Schematic of the columns; (● ) Oxygen concentration sensor, (■ ) Water content sensor, (■ ) volcanic ash, and (▩ ) river sediment (All units are in mm.)

#### 2.2.3.2. **Column setup**

The physical properties of the packed layers are listed in Table 2.1. The packing of the crushed rock sample in all the columns was standardized by compacting 679 g of the air-dried rock to a thickness of 5 cm. In the cases of columns with additional layer(s), the river sediment or volcanic ash was packed to a bulk density of 1.35 g/cm$^3$. Three sensors were installed inside each column. Two of them were responsible for measuring volumetric water content (Θ) (WD-3, ARP Corporation, Japan), and the other sensor was used for detecting $O_2$ concentration (MIJ-03, Environmental Measurement Japan Corporation, Japan). The $O_2$ concentration sensor was placed between the two water content sensors, which were located at a depth of 5 and 15 cm from the top of the crushed rock layer as shown in Fig. 2.1. These sensors simultaneously recorded the data every 10 min and sent the real-time change of data to a data logger (FT2-CTRL, M.C.S. Corporation, Japan) throughout the experiments.

#### 2.2.3.3. **Irrigation and collection of effluent**

Distilled water was irrigated via a rainfall simulator to mimic actual rain. Every week, 200 mL of distilled water, equivalent to the average rainfall in Hokkaido, was poured at once to the rain fall simulator at the top of each column, and it gravitationally infiltrated to the packed layer, representing a heavy rainfall (Ministry of Land Infrastructure Transport and Tourism Japan 2010). This irrigation corresponds to the worst case scenario in terms of As leaching (Tabelin et al. 2012a). Effluents were collected at the bottom of each column by using a 250-mL polypropylene bottle. Since the columns were initially dried, a time lag between the first irrigation and the first collection was observed. In case 1, the first effluent sample was collected on the 3$^{rd}$ week. In contrast, in cases 2, 3, and 4, the first effluents were obtained in the 4$^{th}$ week. The longer time lag was observed in cases 2, 3, and 4 because of the presence of additional layer(s) resulting in larger pore volume (PV) or larger space for holding the irrigated water. After the first collection, effluents were regularly collected once a week before the next irrigation. Once obtained the effluents, pH, ORP, and EC of the liquid sample were immediately measured, then filtered using 0.45-μm Millex® filters, and stored in an air-tight polypropylene bottle prior to chemical analysis.

Table 2.1 Initial conditions of column experiments

| Column number | Irrigation volume (ml/week) | Excavated rock layer | | | Additional layer(s) | | | | | |
|---|---|---|---|---|---|---|---|---|---|---|
| | | Bulk density (Air-drying) ($g/cm^3$) | Porosity (%) | Hydraulic conductivity (m/s) | Material | Bulk density (Air-drying) ($g/cm^3$) | Porosity (%) | Hydraulic conductivity (m/s) | Covering layer | Adsorption layer |
| 1 | 200 | 1.62 | 41 | $6.8\times10^{-6}$ | - | - | - | | No | No |
| 2 | 200 | 1.62 | 41 | $6.8\times10^{-6}$ | Volcanic ash | 1.35 | 55.8 | $1.68\times10^{-6}$ | No | Yes |
| 3 | 200 | 1.62 | 41 | $6.8\times10^{-6}$ | Volcanic ash | 1.35 | 55.8 | $1.68\times10^{-6}$ | Yes | Yes |
| 4 | 200 | 1.62 | 41 | $6.8\times10^{-6}$ | River sediment | 1.35 | 48.7 | $8.35\times10^{-5}$ | Yes | Yes |

### 2.2.4. Chemical analysis of effluents

Inductively coupled plasma atomic emission spectrometer (ICP-AES) (ICPE-9000, Shimadzu Corporation, Japan) was used to quantify the concentration of elements. A hydride generation technique was applied to determine As concentration. This technique required a process of pre-treatment in which 10 mL of sample was mixed with 3 mL of 12 M HCl, 0.66 mL of 20% of potassium iodide solution, 0.33 mL of 10% of ascorbic acid solution, and 0.66 mL of deionized water (Tabelin et al. 2012b). Reagent-grade chemicals were used in the analysis. Note that an error of 2–3% was found in ICP-AES while the hydride generation technique had 5% inaccuracy. Concentrations of coexisting ions were quantified by cation and anion chromatographs (ICS-1000, Dionex Corporation, USA). Bicarbonate ion ($HCO_3^-$) was analyzed by titration with 0.01 M sulfuric acid ($H_2SO_4$) solution.

## 2.3. Results and Discussion

### 2.3.1. Properties of solid samples

Chemical composition and mineral constituents of the bulk-excavated rock, river sediment, and volcanic ash are listed in Tables 2.2 and 2.3, respectively. The content of As in the bulk-excavated rock was 23.6 mg/kg, which is two times higher than the global average content in sedimentary rocks (Webster 1999). This confirms that this waste rock can potentially release significant amounts of As into the environment. The majority of As resulted from geothermal fluid alterations (Takahashi et al. 2011). Many different types of minerals were identified in the rock as illustrated in Table 2.3. The rock was composed of quartz as a primary mineral; feldspar as the second highest; minor minerals of calcite, chloride, and kaolinite; and a trace amount of pyrite. The presence of calcite can affect the pH of leachate because dissolution of calcite generates $HCO_3^-$, which becomes a buffer solution (Deutsch 1997; Morse et al. 2007). Even though a trace amount of pyrite was found in the excavated rock, oxidation of pyrite can be suspected as a major source of As. This assumption was made from the fact that pyrite was oxidized after exposure to the atmosphere, and therefore, most of the exchangeable fraction in the rock probably originated from the oxidation of pyrite during the exposure to the environment for about 6 months before sampling (Schaufuß et al. 1998). On the other hand, the As content in the river sediment was low and close to the average content of geogenic As (Smedley and Kinniburgh 2002). In contrast, the volcanic ash contains the highest amount of As among all solid samples. The majority of As was found in the residual phase, which was not likely to leak. This fact was confirmed by a very low leaching concentration of As (<1 μg/L) in the batch leaching test. The river sediment and volcanic ash mainly contained silicate mineral with substantial amounts of $Al_2O_3$ and $Fe_2O_3$, having an

adsorption potential for removing As (Ghosh and Yuan 1987; Wang and Mulligan 2006; Cornelis et al. 2008).

Table 2.2 Chemical composition of bulk excavated rock, river sediment, and volcanic ash

| | Rock | River sediment | Volcanic ash |
|---|---|---|---|
| $SiO_2$ (wt.%) | 58.7 | 55.3 | 57.6 |
| $TiO_2$ (wt.%) | 0.82 | 0.81 | 0.9 |
| $Al_2O_3$ (wt.%) | 14.4 | 15.2 | 19.1 |
| $Fe_2O_3$ (wt.%) | 6.22 | 6.97 | 8.7 |
| MnO (wt.%) | 0.07 | 0.13 | 0.11 |
| MgO (wt.%) | 3.49 | 2.02 | 1.4 |
| CaO (wt.%) | 3.31 | 1.75 | 0.9 |
| $Na_2O$ (wt.%) | 1.31 | 1.35 | 1.1 |
| $K_2O$ (wt.%) | 3.22 | 1.73 | 1.3 |
| $P_2O_5$ (wt.%) | 0.13 | 0.07 | 0.029 |
| S (wt.%) | 0.2 | < 0.01 | < 0.01 |
| As (mg/kg) | 23.6 | 0.9 | 31.8 |
| LOI (wt%) | 6.26 | 6.3 | 8.99 |
| Organic C (wt%) | 0.23 | < 0.01 | < 0.01 |
| Water (wt%) | 1.10 | 1.12 | 2.23 |

Table 2.3 Mineralogical composition of rock sample, river sediment, and volcanic ash

| | Excavated rock | River sediment | Volcanic ash |
|---|---|---|---|
| Quart | +++ | +++ | +++ |
| Feldspar | ++ | ++ | ++ |
| Kaolinite | + | | |
| Calcite | + | | |
| Chlorite | + | | + |
| Pyrite | - | | |
| Cristobalite | | | + |
| Smectite | | | + |

+++: High; ++: Medium; +: low; -: Trace.

The physical properties of the solid samples are summarized as listed in Table 2.1. These samples were classified as a semi-permeable material because the hydraulic conductivity was in the range of $10^{-5}$–$10^{-6}$ m/s, suggesting that the volcanic ash and river sediment are ideal to be used as covering and adsorption layers in terms of permeability. Figure 2.2 shows the results of the zeta potential of the river sediment and volcanic ash as a function of pH. Although the river sediment and volcanic ash had negative surface charge in a wide range of pH (2–12), these two samples were selected as an adsorption layer.

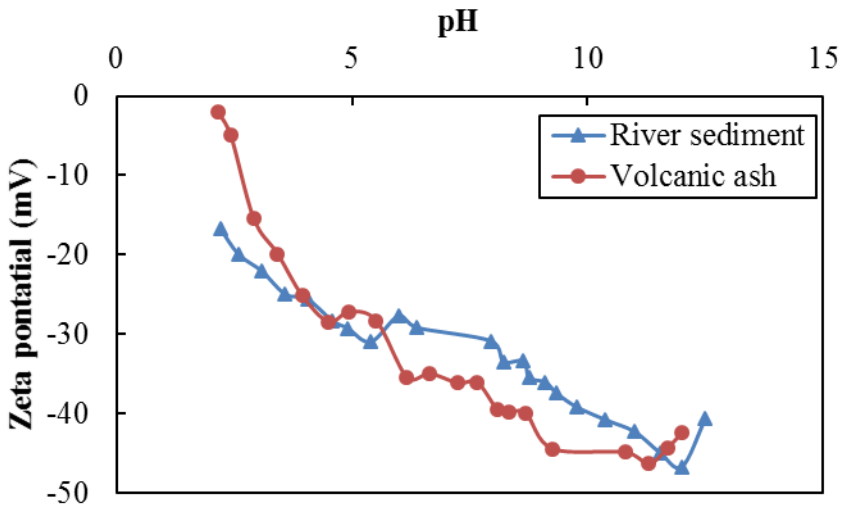


Figure 2.2 Zeta potential vs pH of river sediment and volcanic ash

### 2.3.2. **Effects of additional layer(s) on water content and oxygen concentration**

Figures 2.3a–d show the change in volumetric water content in cases 1 to 4. Some missing points of water content in case 1 were observed due to a sensor failure. Water content in all the columns was initially around 0.2 since the air-dried samples were packed. During the first few weeks, after irrigation in all the cases, the water content rapidly increased, and then remained at higher water content of around 0.3 to 0.4, demonstrating the accumulation of water inside the columns. The water content at a deeper rock layer in case 1 was slightly decreased after each irrigation for the first few weeks whereas the water content in the other cases became almost constant regardless of the irrigation. This is probably due to the water retention characteristics of additional layer(s) in cases 2 to 4; covering and adsorption layers can help to prevent rapid evaporation and percolation of water from the rock layer, respectively.

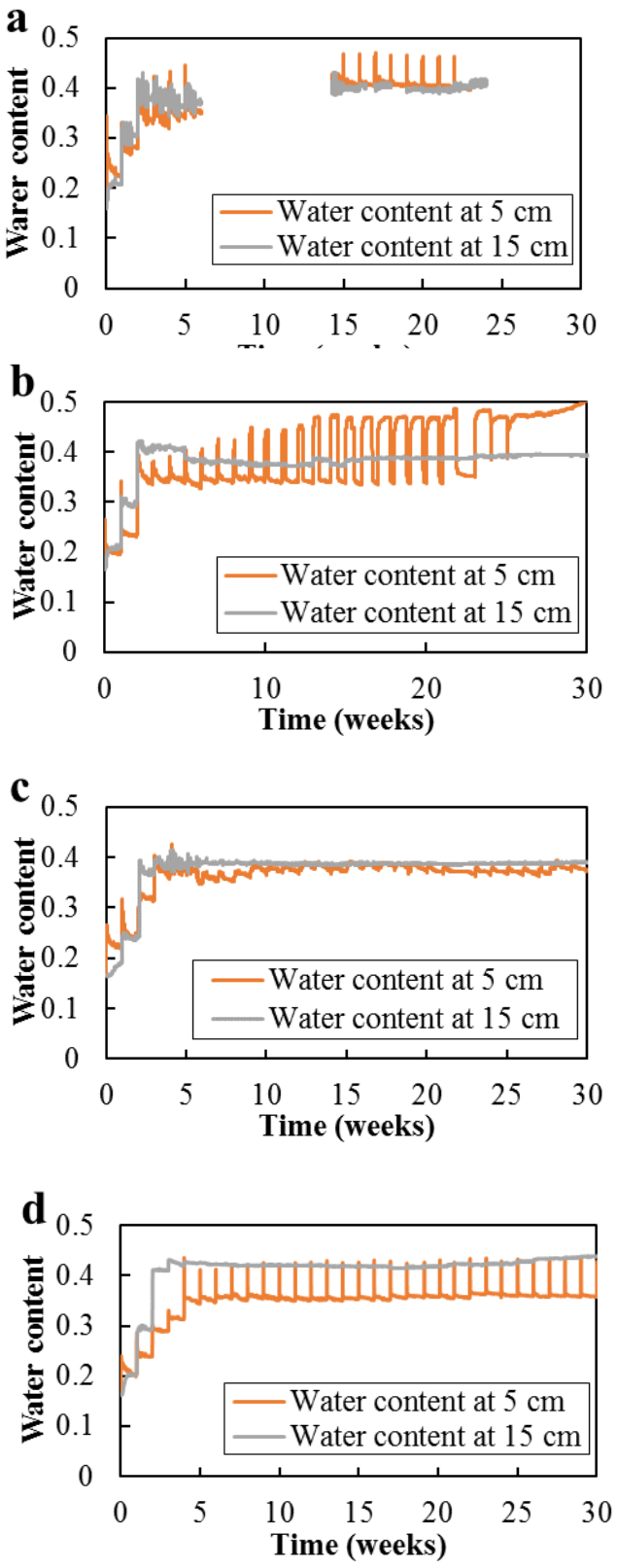


Figure 2.3 Changes in water content; (a) Case 1, (b) Case 2, (c) Case 3, and (d) Case 4

The average evaporation rate was determined by the mass balance calculation as shown in Equation (2.1).

Evaporation rate = 200 - mass of effluent (ml/week) (2.1)

The calculation was done at the point where water was no longer accumulated inside the columns. In case 2, the result cannot be obtained due to the development of clogging water pathways in the column. The average evaporation rate in case 1 was 14.5 mL/week. In contrast, the rate was reduced to 9.6 and 12.2 mL/week in cases 3 and 4, respectively. These results indicate the reduction of evaporation by the covering layer. Although the highest evaporation rate was found in case 1, it was still low and insignificant compared to the weekly irrigation (200 mL).

In all the columns, as time elapsed, the shallower water content fluctuated in accordance with weekly irrigation while almost constant water content was observed in the deeper layer. These results indicate that the water content in the upper rock layer was unsaturated whereas the water content in the lower layer was almost saturated. Generally, the volumetric water content in the shallower layer should not exceed the content in the deeper layer. However, the inverse trend can be seen in some data points of cases 1 and 2 (Fig. 2.3a, b). This was probably due to the looser packing of rock around the shallower sensors when fixing the sensors in the columns. The degree of fluctuation of the shallower water content in case 3 was less drastic than those in cases of 1, 2, and 4, probably due to the lower porosity around the sensor. However, the nearly saturated zone in the deeper rock layer was expected to be more significant in cases 2, 3, and 4 than case 1 due to the presence of the adsorption layer in those cases. Moreover, in case 2, a flat peak of the signal from the shallower sensor was observed from week 9, indicating larger development of the zone with almost saturated water content, caused by development of clogging water pathways in the column.

Figure 2.4 shows the change in $O_2$ concentration in cases 1 to 4. The $O_2$ sensors used in this experiment can detect $O_2$ concentration in both gaseous and aqueous phases. Initial $O_2$ concentration was approximately 21% in all the cases, which is equivalent to the average ambient concentration of $O_2$. Except for case 1, the amount of $O_2$ gradually decreased before the first collection. After the water content at the deeper rock layer approached saturation, $O_2$ concentration dramatically decreased and reached almost zero at week 6 in cases 2 and 3, and at week 10 in case 4. On the other hand, in case 1, $O_2$concentration gradually decreased until week 10 before exponentially decreasing and reaching almost zero at week 15. These results clearly indicate a negative correlation between $O_2$ concentration and volumetric water content, meaning that the faster the accumulation of water, the faster the reduction of $O_2$ concentration.

A delay in the reduction among them was observed, which is possibly due to the effects of the adsorption and covering layers. It was only the rock layer in case 1 (without covering and adsorption layers) that led to the slowest accumulation of water among all the cases. This resulted in high $O_2$ concentration during the first 10 weeks before decreasing to almost zero. Moreover, the $O_2$ concentration was affected not only by water replacement but also by the oxidation of sulfide minerals in the rock. This observation was supported by the slight reduction of $O_2$ concentration at the position where water content was already stable.

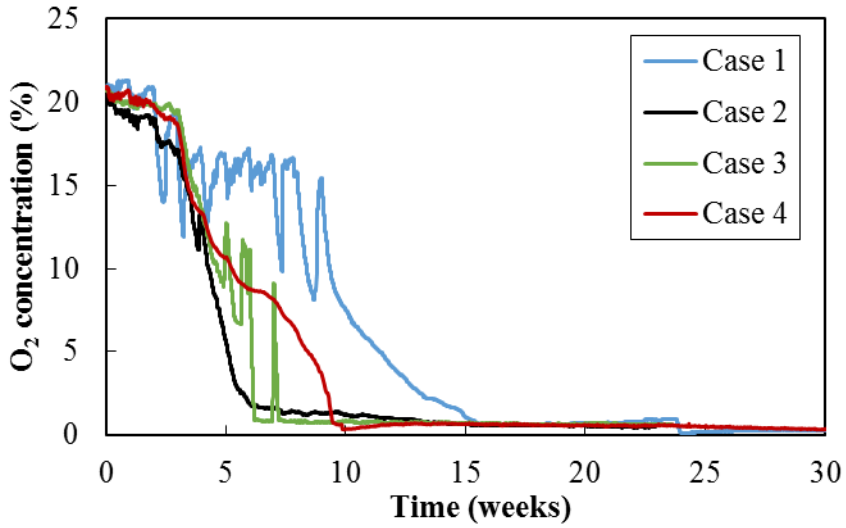


Figure 2.4 Changes of oxygen concentration

### 2.3.3. **Effects of additional layer(s) on pH, Eh, EC, and coexisting ions**

The pH values in all the cases ranged between neutral and moderately alkaline as shown in Fig. 2.5a. This variation in pH could be mainly attributed to three processes, including pyrite oxidation, precipitation of Fe oxy-hydroxide/oxide, and dissolution of calcite.

The aqueous pyrite oxidation generally occurs according to the following chemical equations (Chandra and Gerson 2010):

$$FeS_2(s)+7/2O_2(aq)+H_2O \Leftrightarrow Fe^{2+}+2H^{+}+2SO_4^{2-} \quad (2.2)$$

$$FeS_2(s)+14Fe^{3+}+8H_2O \Leftrightarrow 15\ Fe^{2+}+16H^{+}+8\ SO_4^{2-} \quad (2.3)$$

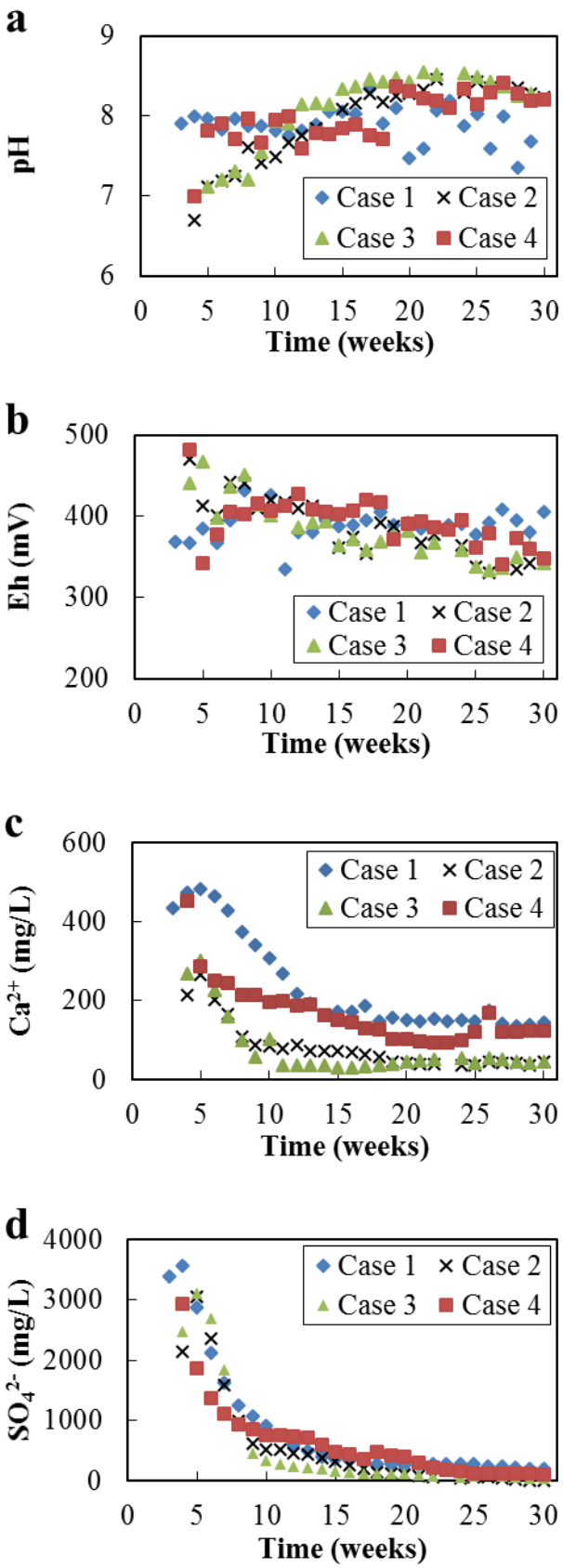


Figure 2.5 Changes in pH, Eh, $Ca^{2+}$, and $SO_4^{2-}$ concentrations with time; (a) pH vs time, (b) Eh vs time, (c) $Ca^{2+}$ concentration vs time, and (d) $SO_4^{2-}$ concentration vs time

Under neutral and moderately alkaline pH, ferrous ($Fe^{2+}$) is rapidly oxidized to ferric ($Fe^{3+}$), and then precipitated as Fe oxy-hydroxide/oxide according to the following reactions (Stumm and Lee 1961; Gupta and Gupta 2005):

$$Fe^{2+}+1/4\ O_2\ (aq)+H^+ \Leftrightarrow Fe^{3+}+1/2H_2O \qquad (2.4)$$

$$Fe^{3+}+3H_2O \Leftrightarrow Fe(OH)_3\ (s)+3H^+ \qquad (2.5)$$

Therefore, pyrite oxidation and precipitation of dissolved Fe are the reactions to lowering the pH of the effluent.

However, calcite dissolution (Equation 2.6) consumes $H^+$ and generates $HCO_3^-$, which has a buffering capacity as a by-product (Lui and Dreybrodt 1997). Therefore, neutral to moderately alkaline pH was observed in all the cases.

$$CaCO_3(s)+H^+ \Leftrightarrow Ca^{2+}+HCO_3^- \qquad (2.6)$$

In cases 1 and 4, the variation of pH was relatively stable ranging between 7.6 and 8.4 throughout the experiment except the pH of the first effluent in case 4. On the other hand, in cases 2 and 3, the pH of effluents was initially low, and then slightly increased and stabilized at around pH 8.2–8.4. Thus, the pH buffering capacity of the volcanic ash and river sediment reduced the pH in cases 2, 3, and 4 at the beginning of the experiment.

In all the cases, Eh was relatively uniform, ranging between 325 and 475 mV as shown in Fig. 2.5b. Thus, the presence of the additional layer(s) did not have a significant effect on the variability of Eh.

Figures 2.5c, d illustrate the leaching behavior of calcium ion ($Ca^{2+}$) and sulfate ion ($SO_4^{2-}$), respectively. In all the cases, the concentrations of $Ca^{2+}$ and $SO_4^{2-}$ were high at first and dramatically decreased before becoming steady. The leaching curve of $Ca^{2+}$ stabilized at around 148, 40, 48, and 115 mg/L in cases 1, 2, 3, and 4, respectively. On the other hand, the concentration of $SO_4^{2-}$ stabilized at the average values of 252, 55, 77, and 176 mg/L. The variation of EC in all the cases was highly correlated with the $Ca^{2+}$ and $SO_4^{2-}$ leaching concentrations as shown in Fig. 2.6a, b, respectively. These correlations suggest that the majority of ions contained in the effluents were $Ca^{2+}$ and $SO_4^{2-}$. Therefore, the flushing-out trends of these ions resulted from calcite dissolution and pyrite oxidation together with the dissolution of soluble phase minerals such as Ca-sulfates (e.g., gypsum) and Fe-sulfates ($Fe_2(SO_4)_3$, Fe $SO_4$), most likely caused by calcite dissolution and pyrite oxidation before

sampling (Chandra and Gerson 2010; Donato et al. 1993; Todd et al. 2003). The stable and low leaching curves of those ions were probably due to the continuation of calcite dissolution and pyrite oxidation. Figure 2.7 illustrates the relationship between molar concentration of $SO_4^{2-}$ and that of $Ca^{2+}$ in the effluent of case 1. The correlation was made at the points where the leaching curves of those ions were stable to avoid the effects of the dissolution of soluble phase minerals. A positive correlation with a molar ratio between $SO_4^{2-}$ and $Ca^{2+}$ of approximately 0.5 was observed. This result indicates that the calcite dissolution and pyrite oxidation occurred simultaneously by ignoring the Equation (2.3) because of weakly alkaline conditions. It can also be confirmed by the relatively stable pH in case 1 since the dissolution of calcite generates $HCO_3^-$, having a buffering capacity to resist lowering pH due to pyrite oxidation (Fig. 2.5a).

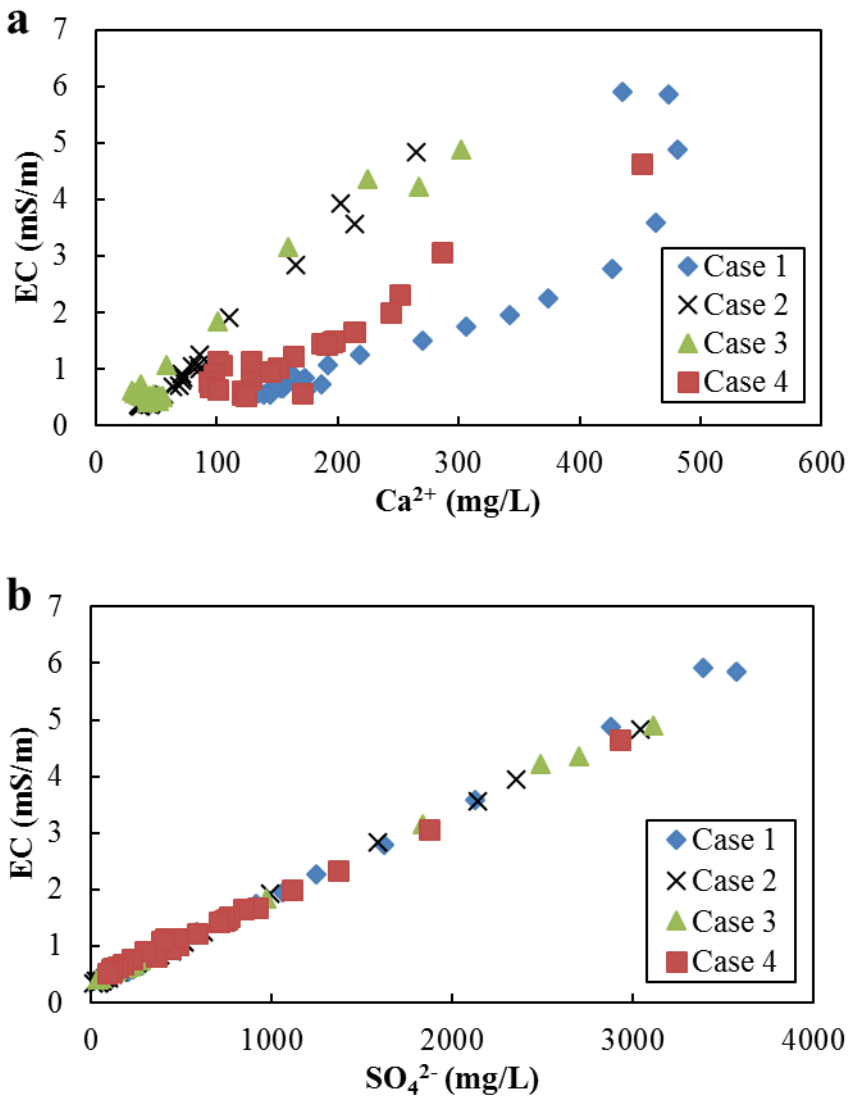


Figure 2.6 Electrical conductivity vs concentrations of (a) $Ca^{2+}$ and (b) $SO_4^{2-}$

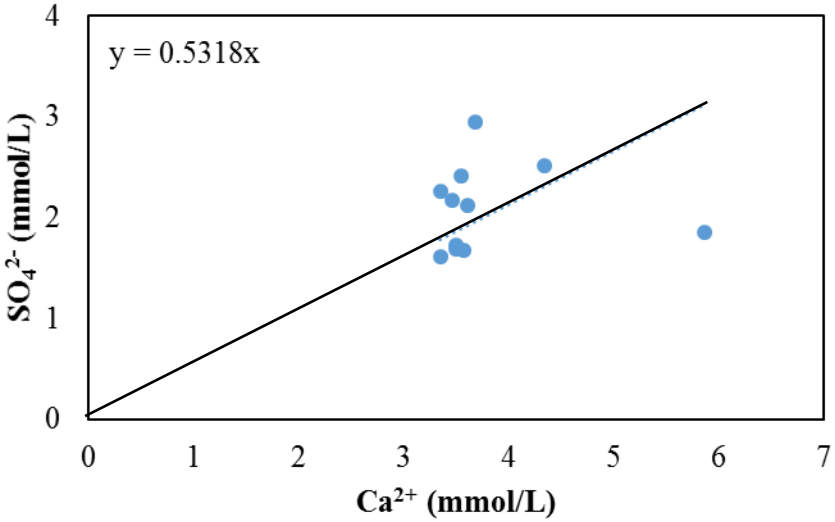


Figure 2.7 Correlation between $SO_4^{2-}$ and $Ca^{2+}$ in case 1

The concentration of $SO_4^{2-}$ in case 1 was the highest during most of the experimental period. This result suggests lower oxidation of pyrite in cases 2, 3, and 4, meaning that the presence of covering and adsorption layers and/or a faster and larger development of the nearly saturated zone in the rock layer plays a role in reducing pyrite oxidation in the rock layer. The lower oxidation of pyrite results from the depletion of aqueous $O_2$ in the rock layer, caused by a lower diffusion of air. As more water accumulates inside the rock, it slows down the air diffusion rate, thereby reducing its $O_2$ load (Aachib et al. 2004; Bornstein et al. 1980; Neira et al. 2015). However, the covering layer did not dramatically influence the pyrite oxidation since the $SO_4^{2-}$ concentration in case 2 was almost identical to that in case 3. This means that the effects of the covering layer on lowering the air diffusion rate was less significant compared to the effects of water accumulation in the rock layer. The reduction in pyrite oxidation might lower calcite dissolution since $H^+$, the product of pyrite oxidation, can be the reactant dissolving calcite (Equation (2.5)). However, the leaching of $Ca^{2+}$ was mainly controlled by the adsorption of $Ca^{2+}$ onto the surface of the adsorption layer due to the negative surface charge. This was confirmed by the highest $Ca^{2+}$ concentration in case 1.

### 2.3.4. **Effects of the additional layer(s) on arsenic release**

Figure 2.8 shows the change of As concentration in the effluent in cases 1 to 4. The As concentration in case 1 was the highest among all the cases and fluctuated between 19 and 38 µg/L throughout the experiment. On the other hand, the leaching concentration of As in case 4 was higher than 10 µg/L during the first 17 weeks before a sudden decrease in week 19 to below 5 µg/L while, in cases of 2 and 3, it was below the drinking water guideline (10 µg/L) except for the leaching of the second effluent in case 2 (WHO 2011). Figure 2.9 illustrates the

correlation between As concentration in the effluents and pH of cases 1 to 4. A positive correlation was observed in case 1 while the opposite trend was found in the other cases. In general, As tends to desorb and become harder to adsorb with increasing pH since surface charges of adsorbents turn to be more negative (Dzombak and Morel. 1990). However, in cases 2 to 4, the negative correlation was obtained, which is due to the role of additional layer(s). As mentioned earlier, the presence of additional layer(s) resulted in faster and larger development of the nearly saturated zone in the rock layer. This plays an important role in reducing the mobilization of As because of the following mechanisms: first, when the water was accumulated within the rock layer, it led to a slower diffusion rate of $O_2$ into the rock layer, and second, the lower $O_2$ concentration decreased oxidation of sulfide minerals, especially pyrite, which resulted in less As released from the rock. Although the adsorption materials had a negative surface charge, these materials also contributed to the reduction of As levels because they contained substantial amounts of $Al_2O_3$ and $Fe_2O_3$ and their own buffering capacity to lower the pH, resulting in increasing As adsorption by the development of a positive surface charge on the adsorbent. The role of the covering layer is generally to limit the intrusion of water and $O_2$ from the surroundings into the rock. However, it could not be clearly determined since the effects of water runoff were restricted by using one-dimensional column experiments. Moreover, the movement of water in the rock layer may also be a potential factor affecting the migration of As. In cases 2 and 3, the longer water retention time in the rock layer caused by lower hydraulic conductivity of the adsorption layer may lead to more precipitation of Fe oxy-hydroxide/oxide. Longer water residence time allows more time for water to dissolve Fe from the dissolvable phase (e.g., $Fe_2(SO_4)_3$) and precipitate as Fe oxy-hydroxide/oxide, producing $H^+$ as a by-product. This might be the result of a very low amount of As leaching in cases 2 and 3 due to the following reasons: the first is that these precipitates have high adsorption affinities toward As (Safiullah et al. 2004; Tabelin et al. 2012a), the second is that As can also be co-precipitated with Fe oxy-hydroxide/oxide (Klerk et al. 2012; Ruiping et al. 2007), and the third is that the higher amounts of these precipitates result in a lower pH, which also enhances the As adsorption.

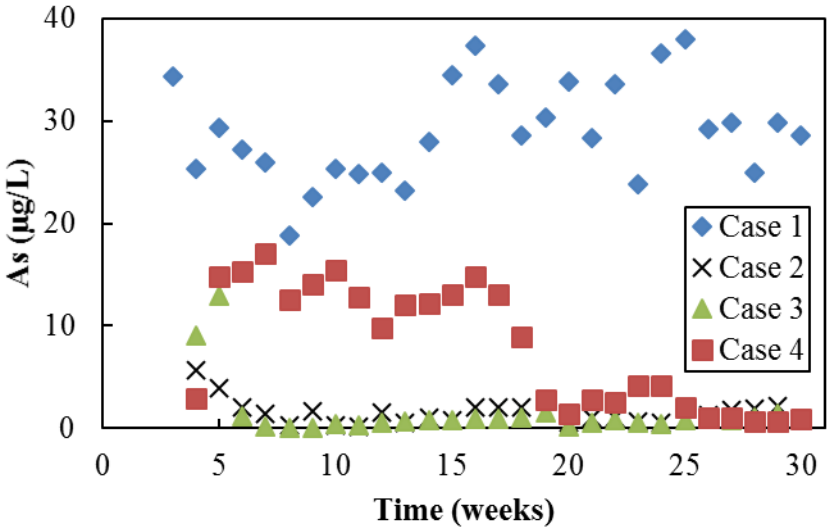


Figure 2.8 Changes in As concentration with time

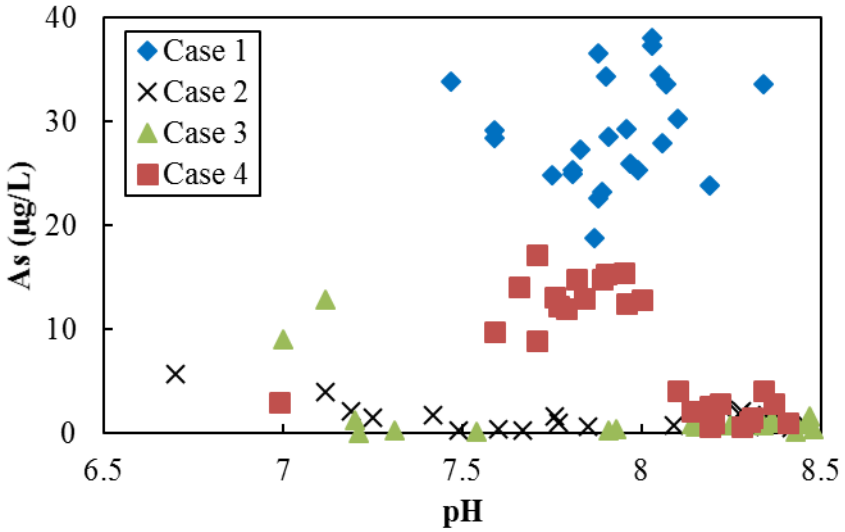


Figure 2.9 As concentration vs pH

## 2.4. **Conclusion**

Four cases of laboratory column experiments were carried out. The replacement of air by water led to a negative correlation between volumetric water content and $O_2$ concentration. The presence of additional layer(s) led to faster and larger development of the zone with higher water content since rapid evaporation and percolation of water from the rock layer were limited by the covering and adsorption layers, respectively. This process resulted in the reduction of oxidation of As-bearing minerals due to slower diffusion of air into pore water. In addition, As was also retarded by the adsorption layer located underneath the rock layer since it contained substantial amounts of Fe and Al oxide. Moreover, a lower water flow rate induced by the use

of covering and adsorption layers with lower hydraulic conductivity compared with the rock layer may lead to higher precipitation of Fe oxy-hydroxide/oxide in the adsorption layer, which has a strong adsorption affinity to As. As a result, the columns with additional layer(s) released significantly lower amounts of As.

## References


Aachib, M., Mbonimpa, M., Aubertin, M. (2004). Measurement and prediction of the oxygen diffusion coefficient in unsaturated media, with applications to soil covers. Water, Air, & Soil Pollution, 156(1), 163–193.

Appelo, C. A. J., Postma, D. (2005). Geochemistry, Groundwater and Pollution (2nd. ed.). London: A.A. Blkema. Bornstein, J., Hedstrom, W. E., Scott, F. R. (1980). Oxygen diffusion rate relationships under three soil conditions. Technical Bulletin, 98, 1–12.

Chandra, A. P., Gerson, A. R. (2010). The mechanisms of pyrite oxidation and leaching: A fundamental perspective. Surface Science Reports, 65(9), 293–315.

Cornelis, G., Johnson, C. A., Gerven, T. V., Vandecasteele, C. (2008). Leaching mechanisms of oxyanionic metalloid and metal species in alkaline solid wastes: A review. Applied Geochemistry, 23(5), 955–976.

Deutsch, W. J. (1997). Groundwater Geochemistry: Fundamentals and Applications to Contamination. Florida: Lewis.

Donato, P., Mustin, C., Benoit, R., Erre, R. (1993). Spatial distribution of iron and sulphur species on the surface of pyrite. Applied Surface Science, 68(1), 81–93.

Dzombak, D. A., Morel, F. M. M. (1990). Surface Complexation Modeling: Hydrous Ferric Oxide. New York: Wiley.

Foster, A. L., Brown, G. E. Jr., Tingle, T. N., Parks, G. A. (1998). Quantitative arsenic speciation in mine tailings using X-ray absorption spectroscopy. American Mineralogist, 83, 553–568.

Ghosh, M. M., Yuan, J. R. (1987). Adsorption of inorganic arsenic and organoarsenicals on hydrous oxides. Environmental Progress, 6(3), 150–157.

Gupta, A. K., Gupta, M. (2005). Synthesis and surface engineering of iron oxide nanoparticles for biomedical applications. Biomaterials, 26(18), 3995–4021.

Katsumi, T., Benson, C. H., Foose, G. J., Kamon, M. (2001). Performance-based design of landfill liners. Engineering Geology, 60(1-4), 139–148.

Klerk, R. J. D., Jia, Y., Daenzer, R., Gomez, M. A., Demopoulos, G. P. (2012). Continuous circuit coprecipitation of arsenic (V) with ferric iron by lime neutralization: Process parameter effects on arsenic removal and precipitate quality. Hydrometallurgy, 111–112, 65–72.

Lui, Z., Dreybrodt, W. (1997). Dissolution kinetics of calcium bcarbonate minerals in $H_2O$–$CO_2$ solutions in turbulent flow: The role of the diffusion boundary layer and the slow reaction $H_2O + CO_2 \leftrightarrow H^+ + HCO_3^-$. Geochimica et Cosmochimica Acta, 61, 2879–2889.

Marumo, K., Ebashi, T., Ujiie, T. (2003). Heavy metal concentrations, leachability and lead isotope ratios of Japanese soils. Shigen Chisitsu 53 (2), 125-146 (in Japanese with English abstract).

Ministry of Land Infrastructure Transport and Tourism Japan (2010). Status of water resources in Japan. http://www.mlit. go.jp/common/001121771.pdf, Accessed 1 September 2016.

Morse, W. J., Arvidson, S. R., Luttge, A. (2007). Calcium carbonate formation and dissolution. Chemical Reviews, 107(2), 342–381.

Neira, J., Ortiz, M., Morales, L., Acevedo, E. (2015). Oxygen diffusion in soils: Understanding the factors and processes needed for modeling. Chilean Journal of Agricultural Research, 75, 35–44.

Ruiping, L., Xing, L., Shengji, X., Yanling, Y., Rongcheng, W., Guibai, L. (2007). Calcium-enhanced ferric hydroxide coprecipitation of arsenic in the presence of silicate. Water Environment Research, 79(11), 2260–2264.

Safiullah, S., Kabir, A., Hasan, K., Rahman, M. M. (2004). Comparative study of adsorption-desorption of arsenic on various arsenic removing materials. Journal of Bangladesh Academy of Sciences, 28(1), 27–34.

Savage, K. S., Tingle, T. N., O'day, P. A., Waychunas, G. A., Bird, D. K. (2000). Arsenic speciation in pyrite and secondary weathering phases, Mother Lode Gold District, Tuolumne Country, California. Applied Geochemistry, 15(8), 1219–1244.

Schaufuß, A. G., Nesbitt, H. W., Kartio, I., Laajalehto, K., Bancroft, G. M., Szargan, R. (1998). Reactivity of surface chemical states on fractured pyrite. Surface Science, 411, 321–328.

Smedley, P. L., Kinniburgh, D. G. (2002). A review of the source, behavior and distribution of arsenic in natural waters. Applied Geochemistry, 17(5), 517–568.

Stumm, W., Lee, F. (1961). Oxygenation of ferrous iron. Industry and Engineering Chemistry, 53, 143–146.

Tabelin, C. B., Igarashi, T. (2009). Mechanisms of arsenic and lead release from hydrothermally altered rock. Journal of Hazardous Materials, 169(1-3), 980–990.

Tabelin, C. B., Igarashi, T., Takahashi, R. (2012a). Mobilization and speciation of arsenic from hydrothermally altered rock in laboratory column experiments under ambient conditions. Applied Geochemistry, 27(1), 326–342.

Tabelin, C. B., Igarashi, T., Yoneda, T. (2012b). Mobilization and speciation of arsenic from hydrothermally altered rock containing calcite and pyrite under anoxic conditions. Applied Geochemistry, 27(12), 2300–2314.

Tabelin, C. B., Igarashi, T., Arima, T., Sato, D. (2014). Characterization and evaluation of arsenic and boron adsorption onto geologic materials, and their application in the disposal of excavated altered rock. Geoderma, 213, 163–172.

Takahashi, T., Fujii, K., Igarashi, T., Kaketa, K., Yamada, N. (2011). Distribution properties and leaching of arsenic by the hydrothermally-altered rocks of Nakakoshi Area, central Hokkaido, Japan. Journal of the Japan Society of Engineering Geology, 52(2), 46–54.

Todd, E. C., Sherman, D. M., Purton, J. A. (2003). Surface oxidation of pyrite under ambient atmospheric and aqueous (pH = 2 to 10) conditions: Electronic structure and mineralogy from X-ray absorption spectroscopy. Geochimica et Cosmochimica Acta, 67(5), 881–893.

Wang, S., Mulligan, C. N. (2006). Natural attenuation processes for remediation of arsenic contaminated soils and groundwater. Journal of Hazardous Materials, 138(3), 459–470.

Webster, J. G. (1999). Arsenic. In C. P. Marshall & R. W. Fairbridge (Eds.), Encyclopedia of geochemistry (pp. 21–22). London: Chapman Hall.

WHO (World Health Organization) (2011). Guidelines for drinking-water quality. 4$^{th}$. edition.

# Chapter 3

# EVALUATION OF WATER MOVEMENT IN A MULTILAYER SOIL PROFILE USING HYDRUS-1D

## 3.1. Introduction

At present, the excavated rocks are frequently disposed by covering with low permeability geomembrane, clay, or composite liners to minimize the contact between the rocks and surrounding environment (Katsumi et al. 2001). These materials, however, are costly and man-made. Therefore, it is necessary to search for an alternative material that is cheap, easy to be found in nature, and has the ability to adsorb As leached from the altered rocks.

In searching new potential materials, a variety of analytical and numerical models have been introduced to evaluate the performance in both saturated and unsaturated conditions (Tabelin et al. 2014; Roy et al. 2014; Kofa et al. 2015; Dale et al. 2016). However, the study on the numerical model of As leaching and transport through the unsaturated porous media is still lacking. The water movement is an important factor influencing solute transport. Unlike the flow of water in saturated media, water movement in unsaturated media is a much complicated, which leads to the use of complicated water flow equation in modeling. This, however, allows us to obtain more accurate prediction. Therefore, before simulating the solute migration, this chapter aims to evaluate the applicability in term of water movement of Hydrus-1D, a software package, in simulating the solute migration from column experiments. The model accuracy was assessed by comparing the observed data with predicted results.

## 3.2. Materials and Methods

### 3.2.1. Experimental methodology

#### 3.2.1.1. Sample collection and preparation

A rock sample called slate was collected from the temporary storage site of a road tunnel construction in Nakakoshi, Hokkaido, Japan. This storage site was built to store the As-rich bulk excavated rock. The rock had been exposed to water or moisture and oxygen for about 6 months before sampling. The sample was taken by using shovels at random points. After collection, the sample was air dried under ambient condition, crushed and sieved with a 2 mm aperture screen in the laboratory. On the other hand, a river sediment sample was collected

from a river located near the construction site. The sediment sample was randomly taken by using shovels. After that, it was brought to the laboratory, air dried, crushed, and sieved to obtain particles with less than 2 mm in diameter.

### 3.2.1.2.**Column experiment**

Figure 1 illustrates a schematic of the column. The column was made from transparent polyvinyl chloride. A rainfall simulator was placed on the top of both columns. It was designed to have small holes to mimic actual rainfall and keep the column from contamination. The crushed rock sample was packed in the column and standardized by compacting it into a bulk density of 1.62 g/cm$^3$. In case of the adsorption and covering layers, a river sediment was packed at the bottom and top of the rock layer with 136.5 g of the sediment to a thickness of 10 mm. Moreover two water content sensors and one oxygen sensor were installed in the rock layer. The water content sensors were placed at depth of 5 and 15 cm from the top of rock layer, respectively, while the oxygen sensor was placed between two water sensors as shown in Fig. 3.1.

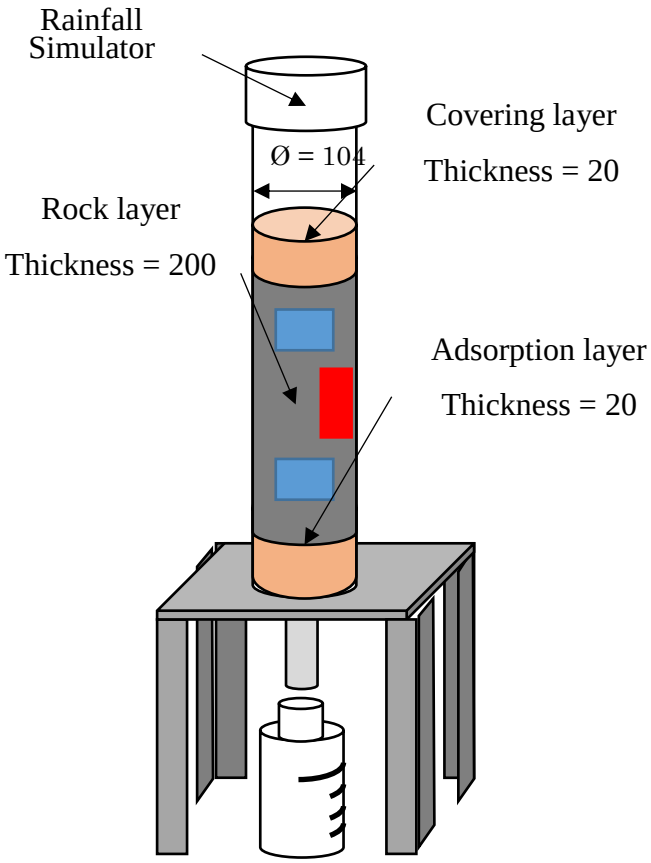


Figure 3.1 Schematic of the column; oxygen concentration sensor (red) and water content sensor (blue) (All units are in mm.)

Distilled water was irrigated to simulate rain. A 200 ml of distilled water was poured every week from the top of the column via a rainfall simulator, which is equivalent to the average rainfall in Hokkaido (1,200 mm/y). Effluent was collected once a week by using a 250 ml polypropylene bottle.

### 3.2.2. **Modeling of water movement**

Hydrus-1D was used to evaluate the transport phenomena of water through the multilayer soil column for a period of 30 weeks. In this study, one-dimensional model could be suitable to describe the flow of water since it was subjected to the transport in column (Simunek et al. 2009).

The movement of water was modeled based on one-dimensional Richard equation as illustrated in Equation (3.1).

$$\frac{\partial\theta}{\partial t} = \frac{\partial}{\partial z}[K(\theta)(\frac{\partial h}{\partial z} + 1)] \quad (3.1)$$

Where $\theta$ is the volumetric water content ($cm^3/cm^3$), $t$ is time (h), $z$ is the vertical axis (cm), $h$ is the matric head (cm), and $K(\theta)$, hydraulic conductivity in vadose zone, is the unsaturated hydraulic conductivity (cm/h). In this simulation, $K(\theta)$ was determined by using the van-Genuchten relationship as shown below:

$$K(\theta) = K_s S_e{}^{l}[1 - (1 - S_e{}^{\frac{1}{m}})^m]^2 \quad (3.2)$$

$$\theta(h) = \theta_r + \frac{\theta_s - \theta_r}{[1+|\alpha h|^n]^m} \quad (3.3)$$

$$m = 1 - \frac{1}{n}, n > 1 \quad (3.4)$$

where the effective saturation ($S_e$) can be determined by:

$$S_e = \frac{\theta - \theta_r}{\theta_s - \theta_r} \quad (3.5)$$

and $\theta_s$ is the saturated water content ($cm^3/cm^3$), $\theta_r$ is the residual water content ($cm^3/cm^3$),

$K_s$ is the saturated hydraulic conductivity (cm/h), and $\alpha$, $n$, and $m$ are fitted parameters determining the shape of the soil water retention curve. The combination of Equations (3.1) through (3.5) describes the one-dimensional water movement in both vadose and saturated zones.

The initial condition was used as a fixed water content, measured by the water content sensors. According to the experimental setup, the irrigated water was forced to flow vertically in one-dimension, surface water runoff was negligible, and a flow system existed as a free-outflow boundary. Thus, the upper boundary condition was selected as the atmospheric boundary with a hypothetical surface layer thicker than the amount of irrigation (>2.4 cm) to represent zero surface water runoff. The lower boundary condition was selected as a seepage face with a specific head.

#### 3.2.2.1. **Model calibration and input parameters**

The matric potential was varied to calibrate the model. Details of the input parameters are listed in Table 3.1. The total quantity of irrigation, evaporation, and accumulation was lumped together as a precipitation term (Equation 3.6) and used as an input.

$$Precipitation = Effluent + Accumulation \quad (3.6)$$

The accumulation term can be determined by the following equation:

$$Accumulation = A\left\{\left[\int_{h_1}^{h_2}\theta_r + \frac{\theta_s-\theta_r}{[1+|\alpha h|^n]^m}dh\right]_f - \left[\int_{h_1}^{h_2}\theta_r + \frac{\theta_s-\theta_r}{[1+|\alpha h|^n]^m}dh\right]_i\right\} \quad (3.7)$$

where $A$ is the cross sectional area of the column ($cm^2$), $h_1$ is the matrix head at the bottom of the column (cm), $h_2$ is the matrix head at the top of the column (cm), and $i$ and $f$ are the initial and final stages in each week, respectively. The van-Genuchten parameters were obtained by fitting the results from a 1-meter height column experiment.

Table 3.1 Input parameters

| Irrigation | Equation (3.6) | |
|---|---|---|
| | **Rock** | **River sediment** |
| Thickness of layer (cm) | 20 | 2 (covering)<br>2 (adsorption) |
| Bulk density (g/cm$^3$) | 1.62 | 1.35 |
| Saturated conductivity (cm/h) | 2.45 | 30.06 |
| van-Genuchten parameters: | | |
| $\Theta r$ | 0.27 | 0.36 |
| $\Theta s$ | 0.44 | 0.487 |
| $\alpha$ | 0.027 | 0.019 |
| $n$ | 6.9 | 4.16 |

## 3.3. **Results and Discussion**

### 3.3.1. **Experimental analysis**

The observed data of volumetric water content in the rock layer at two difference depths are shown in Fig. 3.2. The water content rapidly increased and stayed at higher content after irrigation during the first few weeks, demonstrating the accumulation of water inside the column. The periodic trend was then approached, illustrating that water was continue accumulation until the steady state was reached. Moreover, the water was accumulated more quickly at the deeper, rather than the shallower, parts of the column, suggested by the rapid development of the steady trend of the lower signal. These phenomenon occurred as a result of the higher hydraulic conductivity of the river sediment than the rock in which it acted as a barrier to prevent rapid movement of water from the rock layer.

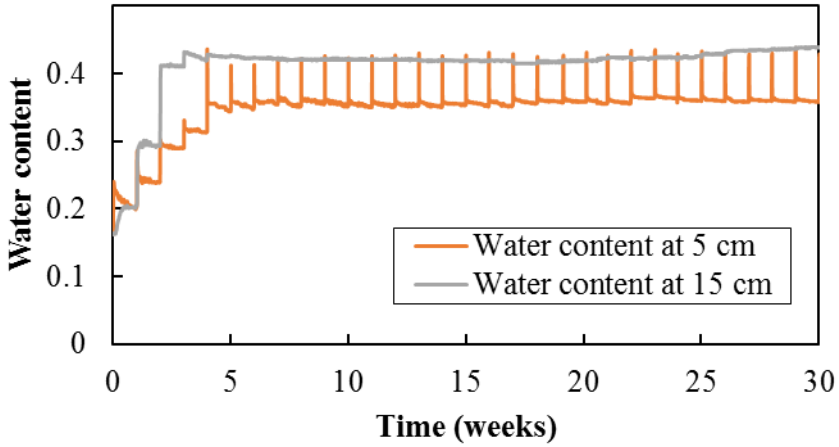


Figure 3.2 Changes in volumetric water content with time

### 3.3.2. **Simulation of water movement**

Water movement was simulated to fit the observed results as illustrated in Fig. 3.3. Hydrus-1D could not simulate the water movement at the beginning of the experiment where the water content was not in the domain of the van-Genuchten equation ($\Theta_r$ = 0.27 and $\Theta_s$ = 0.44). However, this did not have a significant effect on the modeling of the solute transport since there was no effluent leaching out from the column during this period. In this experiment, water was first irrigated to air-dried samples and thus it was just filled the pores from the air-dried to field capacity ($\Theta_r$) conditions before it started to move gravitationally out of the column (SSSA 1997). Most of the observed values matched well with the simulated results from the point where the water content was within the range of $\Theta_r$ and $\Theta_s$. The higher observed data from the lower sensor during the first few weeks probably occurred due to an effect of the unequal hydraulic conductivity of the rock and river sediment. This caused the water to continue accumulating in the rock layer to some extent before flowing down to the layer of river sediment. The inaccurate prediction at the end of the simulation may occurr due to the development of clogging water pathways at the layer below the lower sensor. Although some differences occurred at the beginning and the end of the simulation, Hydrus-1D could predict the transient water movement with high accuracy most of the time. This suggests the capability of Hydrus-1D in simulating the reactive solute transport with accurate transient water movement.

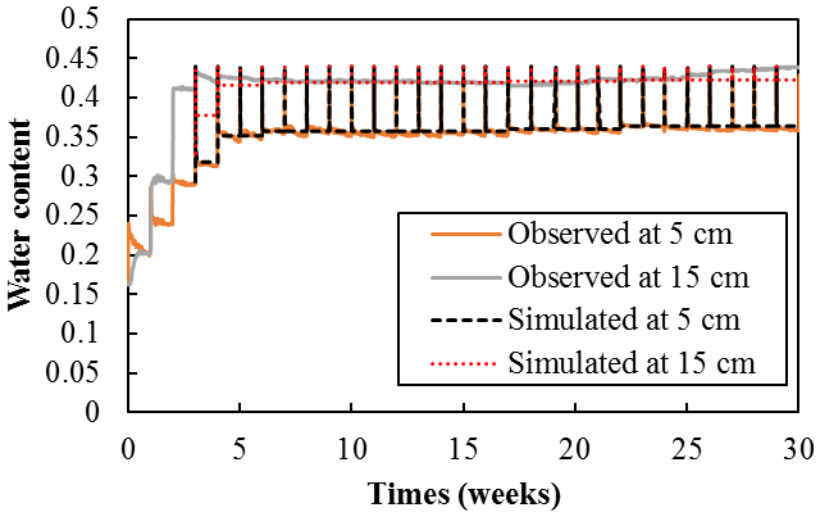


Figure 3.3 Simulation of water movement using Hydrus-1D

## 3.4. **Conclusion**

Water movement is one of the important factors controlling solute transport. Simulations of water movement through multilayer unsaturated porous media were carried out using Hydrus-1D to examine the capability of this software package in simulating the solute migration from column experiments. Based on the observed and predicted data, Hydrus-1D successfully modeled the transient water movement with high level of accuracy. Therefore, this computer simulation program is capable of simulating the reactive solute transport with accurate water movement.

## References

Dale, S., Markovski, J., Hristovski, K. D. (2016). Modeling packed bed sorbent systems with the Pore Surface Diffusion Model: Evidence of facilitated surface diffusion of arsenate in nano-metal (hydr)oxide hybrid ion exchange media. Science of The Total Environment, 563-564, 965-970.

Katsumi, T., Benson, C. H., Foose, G. J., Kamon, M. (2001). Performance-based design of landfill liners. Engineering Geology, 60(1-4). 139-148.

Kofa, G. P., NdiKoungoua, S., Kayema, G. J., Kamgab, R. (2015). Adsorption of arsenic by natural pozzolan in a fixed bed: Determination of operating conditions and modeling. Journal of Water Process Engineering, 6, 166-173.

Roy, P., Mondai, N. K., Das, K. (2014). Modeling of the adsorptive removal of arsenic: A statistical approach. Journal of Environmental Chemical Engineering, 2(1), 585-597.

Simunek, J., Sejna, M., Saito, H., Sakai, M., van Genuchten, M. Th. (2009). The HYDRUS-1D software package for simulating the one-dimensional movement of water, heat, and multiple solutes in variably-saturated media version 4.08. Department of Environmental Sciences, University of California Riverside, California.

SSSA. (1997). Glossary of Soil Science Terms 1996. Soil Science Society of America: Madison.

Tabelin, C. B., Igarashi, T., Arima, T., Sato, D., Tatsuhara, T., Tamoto, S. (2014). Characterization and evaluation of arsenic and boron adsorption onto natural geologic materials, and their application in the disposal of excavated altered rock, Geoderma, 213, 163-172.

# Chapter 4

# MODELING AND EVALUATING THE PERFORMANCE OF RIVER SDIMENT ON IMMOBILIZING ARSENIC FROM HYDERTHRMALLY ALTERED ROCK IN LABORATORLY COLUMN EXPERIMENTS WITH HYDRUS-1D

## 4.1. Introduction

The previous chapter evaluated the capability of Hydrus-1D on modelling water movement, and discussed the transport phenomena of water in the column with a multilayer soil profile. In this chapter, after approving the capability of Hydrus-1D, performance of the unsaturated river sediment on immobilizing As from hydrothermally altered rock is evaluated. In order to achieve this, laboratory column experiments were carried out, and Hydrus-1D was used to simulate the solute transport through the unsaturated adsorbent with the input of water movement from chapter 3. The characteristics of As migration through the unsaturated adsorbent was assessed based on experimental and simulation results. This study would help in the development of a sustainable way of disposing the hazardous waste rocks.

## 4.2. Materials and Methods

### 4.2.1. Experimental methodology

#### 4.2.1.1. Sample collection, preparation, and characterization

Solid samples used in this study were identical to those used in the previous chapter. The excavated rock and river sediment were collected from the interim storage of a road tunnel construction site located in the north-eastern part of Hokkaido, Japan and a river nearby the construction site, respectively. Both samples were randomly collected using shovels, brought to the laboratory, dried under an ambient condition, crushed, sieved through a 2 mm aperture screen, and kept in air-tight containers prior to usage, to minimize further oxidation.

X-ray fluorescence spectrometer (XRF) (Spectro Xepos, Rigaku Corporation, Japan) and X-ray diffractometer (XRD) (MultiFlex, Rigaku Corporation, Japan) were used to characterize the chemical and mineralogical compositions, respectively. Sequential extraction was performed to determine the leachability of As from the excavated rock. The procedure was the same as the work by Marumo et al. (2003).

#### 4.2.1.2. **Column experiments**

The schematic diagram of the experimental setup and physical properties of the packed materials in the columns are illustrated in Fig. 1 and Table 1, respectively. Two cases of the column experiment were built and placed under ambient conditions inside the laboratory. The solid samples were homogenized before packing. The bulk density of each sample was standardized by packing an equal amount of weight to the same height. Case 1 was packed with only hydrothermally altered rock and served as a control. In case 2, covering and adsorption layers were placed above and below the rock layer, respectively. In this study, river sediment was used as the additional layers. Three sensors were introduced into the rock layer in each column. Two of them were water content sensors, installed at a depth of 5 and 15 cm from the top of the rock layer. The other sensor was responsible for measuring the oxygen level, located between the two water content sensors. Based on the mean annual rainfall of Hokkaido, 200 ml of distilled water was irrigated weekly through a rain fall simulator that was located on the top of the column to simulate natural rain (Ministry of Land, Infrastructure, Transport and Tourism Japan 2010). Then, the water flowed down and accumulated on the surface of the packed layer before infiltrating through the packed layer by gravitational force. This represents the worse-case scenario of a day with heavy rainfall with respect to the leaching of As (Tabelin et al. 2012). At the bottom of each column, a polypropylene bottle was used to collect effluent. The effluents were collected once a week before the next irrigation. Then, pH, EC, and ORP were measured before filtration with 0.45 µm Millex® filters. Finally, the filtrates were kept in air-tight containers prior to chemical analysis. The column experiments were conducted for 30 consecutive weeks.

#### 4.2.1.3. **Batch leaching experiments**

After 30 weeks of experimentation, all columns were disassembled. The rock layer was divided into 4 equal portions (5 cm thick) while both covering and adsorption layers were sectioned in half (1 cm thick). Then, the sectioned samples were air dried under ambient conditions and separately kept in air-tight containers prior to the leaching experiments. The leaching experiments were conducted by mixing 3 g of the solid sample with 100 ml of 1 M hydrochloric acid (HCl) at 200 rpm for 2 hours. The suspensions were then filtered using 0.45 µm Millex®filters (Merck Millipore, USA). Finally, all filtrates were stored at 6º C prior to chemical analysis.

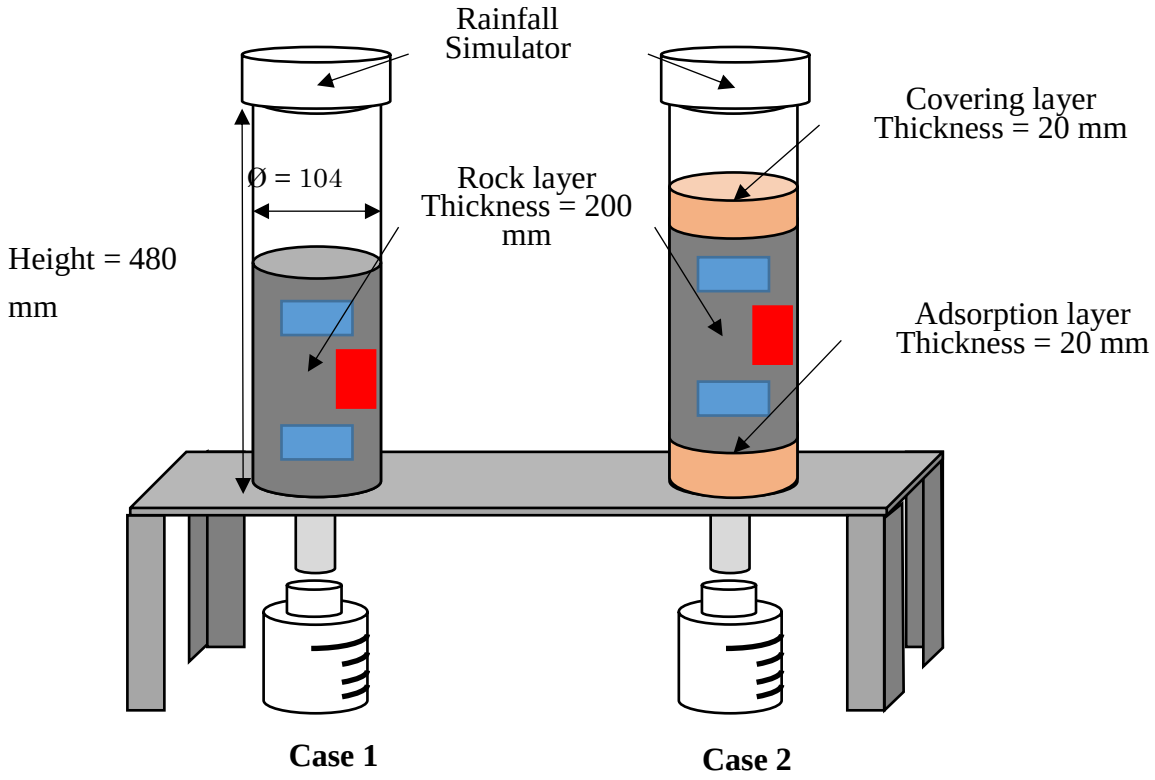


Figure 4.1 Schematic diagram of columns with and without additional layers; ( ) Oxygen concentration sensor, ( ) Water content sensor, and ( ) river sediment

#### 4.2.1.4.**Chemical analysis of liquid samples**

Metal and metalloid concentrations were quantified by ICP-AES (ICPE-9000, Shimadzu Corporation, Japan). The hydride generation technique was used to determine the concentration of As since the As concentration was lower than the detection limit of the standard method (0.1 mg/L). Filtrate samples for hydride generation were prepared by mixing 10 ml of sample with 3 ml of 12 M HCl, 0.66 ml of 20% of potassium iodide solution, 0.33 ml of 10% of ascorbic acid solution, and 0.66 ml of deionized water. All chemicals used in the preparation were reagent-grade. Coexisting ions were also analyzed by cation and anion chromatographs (ICS-1000, Dionex Corporation, USA).

Table 4.1 Physical properties of packed layers

| Column number | Excavated rock | | | River sediment | | |
|---|---|---|---|---|---|---|
| | **Bulk density (air-drying) ($g/cm^3$)** | **Porosity (%)** | **Hydraulic conductivity (cm/h)** | **Bulk density (air-drying) ($g/cm^3$)** | **Porosity (%)** | **Hydraulic conductivity (cm/h)** |
| 1 | 1.62 | 41 | 2.45 | – | – | |
| 2 | 1.62 | 41 | 2.45 | 1.35 | 48.7 | 30 |

### 4.2.2. **Modeling of arsenic migration**

Hydrus-1D was used to evaluate the transport phenomena of As through an unsaturated adsorption layer. This software is capable of simulating a one-dimensional flow of water, heat, and solute in both saturated and unsaturated media (Simunek et al. 2008). One-dimensional model was applied to evaluate the water flow and solute migration (Simunek et al. 2009) because the column experiments expressed one-dimensional phenomena.

The simulation was carried out only in case 2 with weekly basis for 30 weeks. The modeling consisted of two parts. The first part dealt only with water movement to find out the leaching profile at the rock and adsorption layers. This part of the simulation had already been done in the last chapter. The leaching profile was then considered as an input to simulate the As transport over the unsaturated adsorption layer in the second part. The equations, initial and boundary conditions, and input parameters using in the solute transport model are listed below.

The As transport through the adsorption layer was simulated using the one-dimensional advection-dispersion with retardation and first-order decay equation.

$$\frac{\partial \theta R c}{\partial t} = \frac{\partial}{\partial z}\left[\theta D^{w} \frac{\partial c}{\partial z}\right] - \frac{\partial q c}{\partial z} + Fc \qquad (4.1)$$

The retardation factor ($R$) is defined by;

$$R = 1 + \frac{\rho K_d}{\theta} \qquad (4.2)$$

where $\rho$ is the bulk density (g/cm$^3$), $K_d$ is the distribution coefficient (linear adsorption isotherm coefficient), $c$ is the solute concentration (mmol/cm$^3$), $D^w$ is the solute dispersion coefficient for the liquid phase (cm$^2$/h), $q$ is the Darcian fluid flux density (cm/h), and $F$ is the first-order decay term (1/h).

The solute transport was simulated with an initial As concentration of zero in the adsorption layer. The upper boundary condition was set for a concentration flux where the concentration of As can be specified. On the other hand, zero concentration gradient (no change in concentration) was chosen as the lower boundary condition since there was no generation or leaked of As along the way from the adsorption layer to the container.

#### 4.2.2.1. Model calibration and input parameters

The model calibration of the solute transport was done by adjusting two parameters including distribution coefficient ($K_d$) and first-order decay constant ($F$). The input parameters used in the model are given in Table 4.2. The irrigation and input concentration of As were considered based on the results from chapter 3 and the average As leaching concentration from case 1 (30 µg/L), respectively. The van-Genuchten parameters were obtained by fitting the results of volumetric water content from a 1-meter height column experiment. The dispersivity of the river sediment was set according to tracer experiments.

Table 4.2 Input parameters

| | |
|---|---|
| Irrigation | Results from chapter 3 |
| Concentration of As (µg/L) | 30 |
| Material | River sediment |
| Thickness of layer (cm) | 2 |
| Bulk density (g/cm$^3$) | 1.35 |
| Saturated conductivity (cm/h) | 30 |
| Dispersivity | 0.2 |
| van-Genuchten parameters: | |
| $\Theta r$ | 0.36 |
| $\Theta s$ | 0.487 |
| $\alpha$ | 0.019 |
| $n$ | 4.16 |

## 4.3. Results and Discussion

### 4.3.1. Properties of solid samples

The chemical compositions and mineralogy of the rock and river sediment are illustrated in Tables 4.3 and 4.4, respectively. The content of As in the excavated rock was high (23.6 mg/kg) with a trace amounts of sulfide minerals. However, significant quantities of As were expected to be present in sulfide minerals (i.e., pyrite). This can be confirmed by the sequential extraction results (Table 4.5). More than 50% of the total As was found in oxidizable fraction (i.e., sulfides and organic matter). Moreover, most of the As in the exchangeable fraction were probably oxidized from the oxidizable fraction during the period it was exposed to the environment before sampling (Chandra and Gerson 2010). Thus, sulfide minerals, such as pyrite, were a potential source of As even though it was detected only in trace amounts in

the rock body. The results from the sequential extraction also clearly show that the waste rock was a potential source of As contamination since almost 80% of total As was in mobilizable phases. On the other hand, the river sediment showed very low As content with substantial amounts of $Al_2O_3$ and $Fe_2O_3$. These metal oxides have been reported by many studies to have an adsorption capacity for As even in very low content (Katsoyiannis and Zouboulis 2002; Safiullah et al. 2004; Thirunavukkarasu and Subramanian 2003; Nguyen et al. 2011). Consequently, this made the river sediment a potential material for using as adsorption and covering layers.

Table 4.3 Chemical composition of bulk excavated rock and river sediment

| | Rock | River sediment |
|---|---|---|
| $SiO_2$ (wt.%) | 58.7 | 55.3 |
| $TiO_2$ (wt.%) | 0.82 | 0.81 |
| $Al_2O_3$ (wt.%) | 14.4 | 15.2 |
| $Fe_2O_3$ (wt.%) | 6.22 | 6.97 |
| MnO (wt.%) | 0.07 | 0.13 |
| MgO (wt.%) | 3.49 | 2.02 |
| CaO (wt.%) | 3.31 | 1.75 |
| $Na_2O$ (wt.%) | 1.31 | 1.35 |
| $K_2O$ (wt.%) | 3.22 | 1.73 |
| $P_2O_5$ (wt.%) | 0.13 | 0.07 |
| S (wt.%) | 0.2 | < 0.01 |
| As (mg/kg) | 23.6 | 0.9 |
| LOI (wt%) | 6.26 | 6.3 |
| Organic C (wt%) | 0.23 | < 0.01 |
| Water (wt%) | 1.10 | 1.12 |

Table 4.4 Mineralogy of bulk excavated rock and river sediment

| | Excavated rock | River sediment |
|---|---|---|
| Quart | +++ | +++ |
| Feldspar | ++ | ++ |
| Kaolinite | + | |
| Calcite | + | |
| Chlorite | + | |
| Pyrite | - | |

+++: High; ++: Medium; +: low; -: Trace.

Table 4.5 Arsenic speciation of the bulk excavated rock

| Phases | % |
|---|---|
| Exchangeable | 17.9 |
| Carbonate | 2.3 |
| Reducible | 2.4 |
| Oxidizable | 55.2 |

### 4.3.2. **Arsenic releasing behavior**

#### 4.3.2.1. **Experimental analysis**

The changes in Eh, pH, and concentrations of As with time in both cases are shown in Figs 4.2a-c. The Eh and pH are the main parameters governing the chemical species of As releasing from hydrothermally altered rock (Dzombak and Morel. 1990; Smedley and Kinniburgh, 2002; Sailo and Mahanta, 2014). Therefore, these parameters have a strong effect on the mobility of As. However, in this study, the Eh and pH of the effluents in both cases were moderately stable. Consequently, mobilization of As due to the change in these parameters should be minimal.

Arsenic concentration in case 1 fluctuated and varied between 19 and 38 µg/L. On the other hand, the leachates in case 2 contained lower As concentration than those in case 1 throughout the experiment. The reduction of the As levels in case 2 occurred due to the following mechanisms:

First, the river sediment located beneath the rock layer effectively adsorbed As since it contains substantial amounts of $Al_2O_3$ and $Fe_2O_3$ (Katsoyiannis and Zouboulis, 2002; Thirunavukkarasu and Subramanian, 2003; Nguyen et al., 2011). Therefore, this contributed to a reduction of As mobilization.

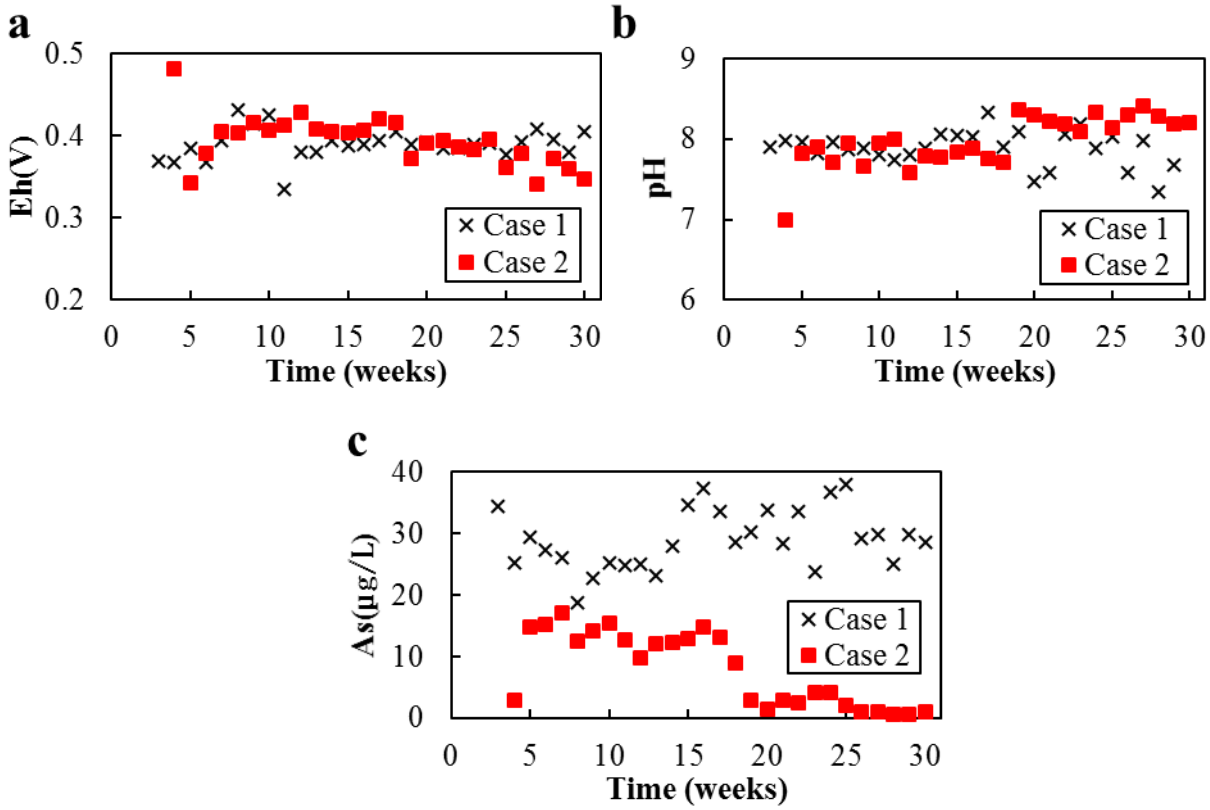


Figure 4.2 Changes in Eh, pH, and As concentration over time: (a) Eh over time, (b) pH over time, and (c) As concentration over time

Second, faster and larger development of nearly saturated zone in the rock layer in case 2 played an important role in reducing the generation of As. Water can significantly lower the $O_2$ level in the rock. Moreover, it can also slow down the diffusion rate of $O_2$ into the rock layer (Bornstein et al. 1980; Aachib et al. 2004; Neira et al. 2015). The occurrence of these phenomena can be confirmed using the observation of volumetric water content and $O_2$ concentration in the rock layer with time in cases 1 and 2 (Figs. 4.3a and b, respectively). During the first few weeks, the water content fluctuated due to rainfall but it generally increased in both cases. In case 2, the increasing trend was stopped after week 5 whereas in case 1 the overall volumetric water content still increased even though seven weeks had passed. This is due to the availability of water content in covering and adsorption layers in case 2, which can act as a barrier to prevent evaporation out of the rock layer. In both columns, the water content at deeper rock layer became constant irrespective of the elapsed time after irrigation. In contrast, the water content at the shallower rock layer was fluctuated throughout the experiment

corresponding to the rainfall. This indicates that the water content at deeper rock layer was almost saturated but at the shallower layer was unsaturated. In addition, the presence of additional layers in case 2 possibly led to the larger saturated zone in the rock layer. On the other hand, initial $O_2$ concentration was about 21% in both columns corresponding to average atmospheric $O_2$ concentration. After distilled water was irrigated, the $O_2$ concentration started to decrease before exponentially dropped to almost zero at weeks 15 and 10 for cases 1 and 2, respectively. Comparing these with the results of volumetric water content, a negative correlation between water contents and $O_2$ concentration is clearly observed. However, a delay response between these two signals might be the result from the difference in the position of the sensors within the column. It can be concluded that the faster and larger accumulation of water in case 2 led to the faster reduction and slower diffusion of $O_2$ in the rock layer. Thus, less As released by oxidation of sulfide minerals is expected.

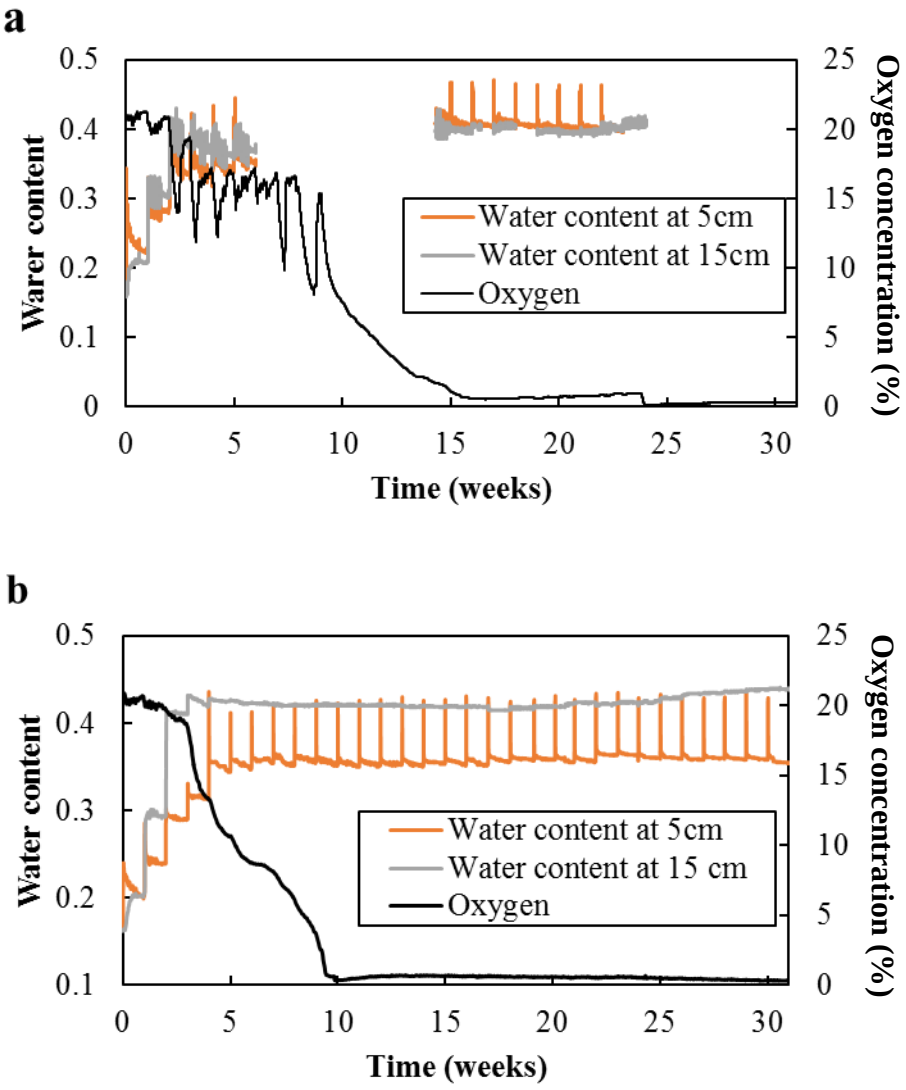


Figure 4.3 Changes in water and $O_2$ concentration; (a) Case 1 and (b) Case 2.

Third is the reduction of As mobilization by new precipitation of Fe oxy-hydroxide/oxide in the adsorption layer. The leaching experiments of the post experimental soil samples were performed to investigate whether or not the precipitation of Fe oxy-hydroxide/oxide was formed and retained inside the column. The leaching concentrations Fe with depth in cases 1 and 2 are shown in Figs. 4.4a and b, respectively. The concentrations of Fe leached from the rock were almost identical in all depths and in both columns, demonstrating no precipitation of Fe oxy-hydroxide/oxide in the rock layer. Meanwhile, the concentration of Fe in the leachates from the adsorption layer was significantly higher than those from the covering layer. Moreover, the highest amount was found at the layer adjacent to the rock. These results confirm the precipitation of Fe oxy-hydroxide/oxide in the river sediment. Consequently, As can be immobilized by co-precipitation with and/or adsorption onto this newly precipitated Fe oxy-hydroxide/oxide (Ruiping et al. 2007; Klerk et al. 2012).

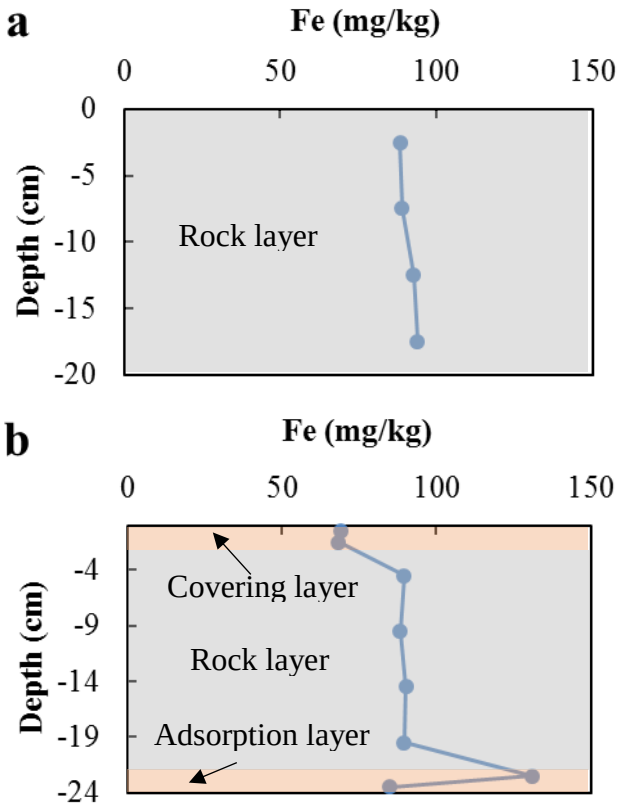


Figure 4.4 Changes in leaching concentration of Fe with depth: (a) case 1 and (b) case 2

#### 4.3.2.2. **Reactive solute transport modelling**

Hydrus-1D was used to simulate the reactive transport of As through the adsorption layer in case 2. The simulation was done by using the advection-dispersion with retardation and first-order decay equation (Equation (4.1)) with an assumption of an equilibrium solute transport model. The equilibrium assumption for the solute transport was made due to the fact

that As concentrations in the effluents collected at four different times during the week were almost identical. In other words, the flow was slow enough for the adsorption to reach equilibrium.

Figure 4.5 shows comparison between simulated results of As migration and observed ones in case 2. The leaching behaviors of As was divided into 3 periods. First, when the level of As rapidly increased during the first few weeks and then fluctuated slightly with the As concentration higher than drinking water standard (10 µg/L) (WHO 2011) prior to week 17 in the second period. In the last period, a sudden decrease of As level occurred and it remained below 5 µg/L. The modeling was done using the default parameters in Table 4.2 and varying two solute transport parameters, $K_d$ and $F$. The values of the fitted parameters at different periods are listed in Table 4.6. First, $F$ was given as a constant equal to 0.01 1/h to adjust the plateau level (at approximately 15µg/L). The $K_d$ was then varied to fit the breakthrough characteristic of As. The value of F remained at 0.01 1/h until week 17 before increasing to 0.06 1/h in which it brought the As concentration down and maintained the leaching concentration at around 3 µg/L from weeks 19 until the end of the simulation.

Table 4.6 Fitted parameters

| **Period** | ***Kd* (ml/g)** | ***F* (1/h)** |
|---|---|---|
| 1st | 10 | 0.01 |
| 2nd | 10 | 0.01 |
| 3rd | 10 | 0.06 |

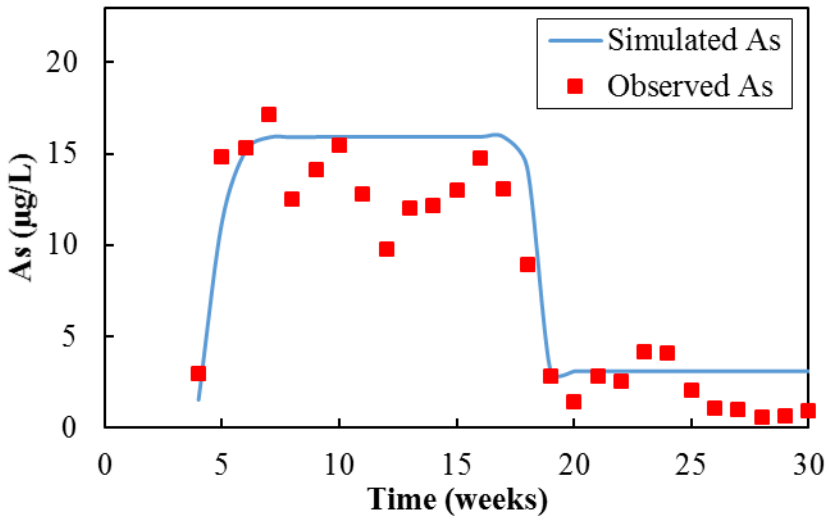


Figure 4.5 Simulation of As breakthrough in case 2 using Hydrus-1D

The simulated results reveal that the mobility of As at the beginning was mainly controlled by $K_d$. Thus, the major mechanism retarding the mobility of As in this period was expected to be a reversible adsorption onto the river sediment. After that, the first-order decay constant played a role in maintaining the leaching concentration of approximately 15 µg/L prior to week 17. This likely represents the depletion of As from such phenomena as faster reduction and slower diffusion of $O_2$ into the rock layer and co-precipitation and adsorption onto newly precipitated Fe oxy-hydroxide/oxide. As time elapsed, the first order decay contributed more significant effect on As releasing behavior. This illustrates further depletion of As likely due to the significantly lower generation by oxidation of sulfide mineral in the rock layer. During this period, the major mechanism of As generation shifted from dissolution to oxidation. This can be explained using the leaching behavior of sulfate ($SO_4^{2-}$), one of the major coexisting ions (Fig. 4.6). The $SO_4^{2-}$ concentration in case 2 exponentially decreased and then stayed stable at low concentration afterwards. The rapid decrease of $SO_4^{2-}$ concentration indicates the release of As from both soluble and oxidizable phases. However, the release of As from the soluble phase decreased with time, suggested by the reduction of a flushing-out trend. Therefore, the combination of the allocation of the As generation mechanism and very low $O_2$ concentration in the rock layer led to a significant reduction of As generation in the last period. In addition, as time elapsed, Fe oxy-hydroxide/oxide continued to precipitate onto the surface of the river sediment, resulting in a higher surface area of the newly precipitated adsorbent over time. Consequently, a higher chance of As being adsorbed onto these newly precipitated materials can be expected

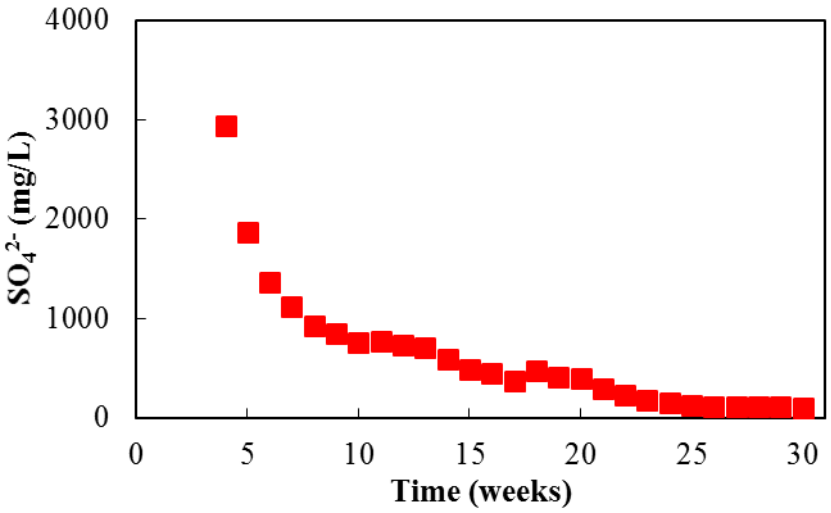


Figure 4.6 Leaching behavior of $SO_4^{2-}$ in case 2

## 4.4. **Conclusion**

Simulations of solute transport through unsaturated porous media were carried out using Hydrus-1D to investigate the performance of the river sediment on immobilizing As from hydrothermally altered rocks. The breakthrough curve of As was fitted by adjusting two solute transport parameters including $K_d$ and $F$. Based on the observed and simulated results, the leaching behavior of As through the river sediment was divided into three periods. Each period had its own mobile characteristics of As. In the first period (weeks 1-5), As was potentially retarded by the adsorption onto the river sediment. From weeks 5-17, the reduction of oxidation of As bearing-minerals, irreversible adsorption, and adsorption of As onto the newly precipitated Fe oxy-hydroxide/oxide probably played a major role on the mobility of As. As time elapsed, the oxidation of As-bearing minerals became more significant since the mechanism of As generation shifted from dissolution to oxidation. Due to this shift, in addition to the low concentration of $O_2$ in the rock layer, the generation of As significantly decreased in the last period. In addition, more As was expected to be adsorbed onto the newly precipitated Fe oxy-hydroxide/oxide since the surface area of these potential adsorbents increased over time. As a result, the river sediment effectively reduced the leaching of As from hydrothermally altered rock.

## References


Aachib, M., Mbonimpa, M., Aubertin, M. (2004). Measurement and prediction of the oxygen diffusion coefficient in unsaturated media, with applications to soil covers. Water, Air, & Soil Pollution, 156(1). 163-193.

Bornstein, J., Hedstrom, W. E., Scott, F. R. (1980). Oxygen diffusion rate relationships under three soil conditions. Technical Bulletin, 98. 1-12.

Chandra, A. P., Gerson, A. R. (2010). The mechanisms of pyrite oxidation and leaching: A fundamental perspective. Surface Science Reports, 65(9), 293–315.

Dale, S., Markovski, J., Hristovski, K. D. (2016). Modeling packed bed sorbent systems with the pore surface diffusion model: Evidence of facilitated surface diffusion of arsenate in nano-metal (hydr)oxide hybrid ion exchange media. Science of The Total Environment, 563-564, 965-970.

Dzombak, D. A., & Morel, F. M. M. (1990). Surface Complexation Modeling: Hydrous Ferric Oxide. New York, Wiley.

Katsoyiannis, I. A., Zouboulis, A. I. (2002). Removal of arsenic from contaminated water sources by sorption onto iron-oxide-coated polymeric materials. Water Research, 36, 5141–5155.

Klerk, R. J. D., Jia, Y., Daenzer, R., Gomez, M. A., Demopoulos, G. P. (2012). Continuous circuit co-precipitation of arsenic (V) with ferric iron by lime neutralization: Process parameter effects on arsenic removal and precipitate quality. Hydrometallurgy, 111-112. 65-72.

Marumo, K., Ebashi, T., Ujiie, T., (2003). Heavy metal concentrations, leachability and lead isotope ratios of Japanese soils. Chisitsu, 53 (2), 125-146 (in Japanese with English abstract).

Ministry of Land, Infrastructure, Transport and Tourism Japan (2010). Status of water resources in Japan. http://www.mlit.go.jp/common/001121771.pdf, Accessed 1 September 2016.

Neira, J., Ortiz, M., Morales, L., Acevedo, E. (2015). Oxygen diffusion in soils: Understanding the factors and processes needed for modeling. Chilean Journal of Agricultural Research, 75. 35-44.

Nguyen, Vu L., Chen, W. H., Young, T., Darby, J. (2011). Effect of interferences on the breakthrough of arsenic: Rapid small scale column tests. Water Research, 45, 4069-4080.

Ruiping, L., Xing, L., Shengji, X., Yanling, Y., Rongcheng W., Guibai L. (2007). Calcium-enhanced ferric hydroxide co-precipitation of arsenic in the presence of silicate. Water Environment Research, 79(11). 2260-2264.

Safiullah, S., Kabir, A., Hasan, K., Rahman, M. M. (2004). Comparative study of adsorption-desorption of arsenic on various arsenic removing materials. Journal of Bangladesh Academy of Sciences, 28(1). 27-34.

Sailo, L., Mahanta, C. (2014). Arsenic mobilization in the Brahmaputra plains of Assam: Groundwater and sedimentary controls. Environmental Monitoring and Assessment, 186, 6805–6820.

Simunek, J., Sejna, M., Saito, H., Sakai, M., van Genuchten, M.Th. (2009). The HYDRUS-1D Software Package for Simulating the One-Dimensional Movement of Water, Heat, and Multiple Solutes in Variably-Saturated Media Version 4.08. Department of Environmental Sciences, University of California Riverside, California.

Smedley, P. L., Kinniburgh, D. G. (2002). A review of the source, behavior and distribution of arsenic in natural waters. Applied Geochemistry, 17(5), 517-568.

Tabelin, C. B., Igarashi, T., Takahashi, R. (2012). Mobilization and speciation of arsenic from hydrothermally altered rock in laboratory column experiments under ambient conditions. Applied Geochemistry, 27(1). 326-342.

Thirunavukkarasu, O. S., Subramanian, T. V. (2003). Arsenic removal from drinking water using iron oxide coated sand. Water, Air, & Soil Pollution, 142. 95-111.

World Health Organization (WHO) (2011). Guidelines for drinking-water quality. 4th edition.

# Chapter 5

# CONCLUSION AND RECOMMENDATION

## 5.1. General Conclusion

This dissertation was conducted with the main objective of evaluating the effects of additional layer(s) on immobilizing As from hydrothermally altered rock. Several laboratory experiments and computer simulations were performed in order to achieve this goal. The contents were divided into five chapters.

In chapter 1, the basic knowledge about As including general properties, effects on human health, sources specifically in rock-forming minerals, common technics to remove aqueous As were reviewed. This chapter also included the basic adsorption theories and general knowledge on modeling of solute migration in a vadose zone. Finally, the objectives and outline of the study were introduced.

Chapter 2 described the relationships of water content and $O_2$ concentration on As leaching behaviors in relation to additional layer(s). Four cases of laboratory column experiment were carried out. Oxygen and water content sensors were installed into the rock layer of every column at the same position. Negative correlation between $O_2$ concentration and volumetric water content was clearly observed due to the replacement of air by water. Additional layer(s) led to faster and larger development of the zone with higher water content. The development of this zone resulted in the reduction of oxidation of As-bearing minerals due to slower diffusion of air into pore water. The adsorption layer located underneath the rock layer also contributed to the retarding of As since it contained considerable amounts of Fe and Al oxide. Moreover, a lower water flow rate caused by the use of low hydraulic conductivity covering and adsorption layers may lead to higher precipitation of Fe oxy-hydroxide/oxide in the adsorption layer. This precipitate was reported by many studies to have abilities to co-precipitate as well as adsorb As. As a result, the columns with additional layer(s) had a significant effect on lowering the migration of As from the rock layer.

Hydrus-1D was used to investigate the water movement and reactive transport of As through an unsaturated adsorption layer in chapters 3 and 4, respectively. In chapter 3, we successfully proved that Hydrus-1D had ability to simulate the reactive transport of As with high level of accuracy in term of transient water movement. In chapter 4, the breakthrough curve of As was fitted by adjusting two solute transport parameters of $K_d$ and $F$. Based on the analysis of experimental and simulation data, the leaching behavior of As through the river

sediment was divided into 3 periods. From weeks 1-5, the As was potentially retarded by the adsorption onto minerals initially contained in the river sediment. The second period, weeks 5-17, the reduction of oxidation of As bearing-minerals, irreversible adsorption, and the adsorption onto newly precipitated Fe oxy-hydroxide/oxide played a major role affecting the mobility of As. In the last period, the major mechanism of As generation shifted to the oxidization of As-bearing minerals. Consequently, the generation of As significantly decreased since the $O_2$ concentration in the rock layer was low. Additionally, the surface area of the newly precipitated Fe oxy-hydroxide/oxide increased over time, resulting in more chance of As to be retarded by these potential adsorbents. In conclusion, significant amounts of As were reduced by the use of river sediment.

## 5.2. **Recommendation**

Dissolution and oxidation are the major mechanisms responsible for As generation from the hydrothermally altered rocks. Therefore, the best countermeasures to restrict the releasing of As is to prevent the occurrence of these two reactions. In other words, these rocks need to be isolated from the atmosphere, in particular, water and $O_2$. This could be done by covering the rocks with low permeable materials. As a precaution in case of covering layer malfunction, a layer of adsorbent is needed to place underneath the rock body to immobilize As. The adsorbent could be either synthetic or natural materials. However, natural adsorbent could be considered more economical. Proper natural adsorbents should contain substantial amounts of metal oxides and/or clay minerals (e.g., kaolinite). Moreover, the adsorption layer should have low permeability to increase the retention time of the contaminant. To achieve this, the large particle of adsorbent should be crushed before use. This will increase adsorption capacity and surface area between contaminant and adsorbent. In addition, more surface area of the adsorbent will lead to higher chance of the deposition of newly precipitated Fe oxide/oxy-hydroxide, by-products from As generation, which can also enhance the immobility of As. It has been known that most of the natural and synthetic adsorbents have the optimum operating pH for retarding As at around neutral. This condition is suitable for adsorption as well as precipitation to occur. Therefore, if the water percolates into the rock layer, it is necessary to keep the pH at around neutral. This could be done by adding layers of neutralizer (e.g., calcite) along the rock layer. The type and amount of neutralizer should be determined in regards to pyrite and calcite ratio of the waste rock since these are the major minerals controlling pH when in contact with water. By considering these recommendations, we are proposing an alternative technique to dispose the hydrothermally altered waste rock. The cross-sectional view of preliminary schematic diagram of the proposed method is shown in Fig. 5.1.

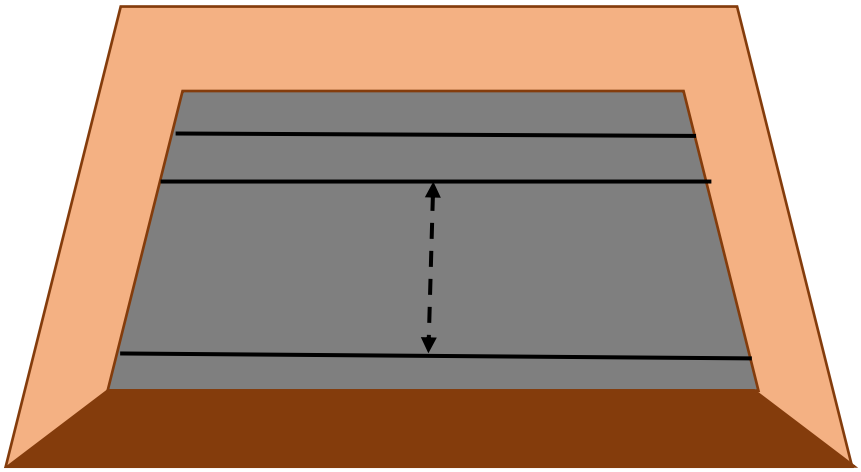

Figure 5.1 Proposed design for disposing hydrothermally altered wasted rock: ( ) low permeable covering material, ( ) low permeable adsorption material, ( - ) neutralizer, and ( ) waste rock

## ACKNOWLEDGEMENT

I would never have been able to finish my dissertation without the guidance of all following person, help from friends, and support from my family.

First of all, I would like to express the highest acknowledgement to my supervisor, Professor Toshifumi Igarashi for giving me a great opportunity to be a part of his laboratory and a chance to study and conduct the interesting research. He also gives me an intellectual guidance, stimulating suggestions, caring, patience, and encouragement. I am also indebted to my thesis committees, Professor Satoru Kawasaki and Professor Masahiro Takahashi, for their kindness, interest, and invaluable advice to my thesis.

I would like to express my sincere gratitude to Assistance Professor Carito Baltazar Tabelin for his insightful advice and patient teaching. Special thanks go to Associate Professor Shusaku Harada, who has been the source of encouragement and enthusiasm, not only during this thesis project but also during three years of my doctoral program.

Particular thank goes to Mr. Ota Jin and Mr. Ritsuto Hayashi, for their excellent technical assistant during my research. Moreover, I would like to thank all members of the laboratory of groundwater and mass transport for their help and encouragement during my research and studies. I have had a great and wonderful research life in Japan because I joined this laboratory.

My greatest appreciation goes to my friends; Dr. Worawan Sornkom, Dr. Ruchirada Changkwanyeun, Ms. Bongkot Soonthornsata, Mr. Buddy de Vos, Mr. Mungman Samakpong, Mr. Harin Leelayuwapan, Mr. Kweepoj Siwanartnusorn, Mrs. Keskaew Srivilairit, and Ms. Nattida Wongratanarutt for their sincere friendship, supporting and valuable suggestion, not only for the research but daily life also. I would never forget all the chats and beautiful moments that I shared with all of them. They are fundamental in supporting me during the stressful and difficult times.

I would like to acknowledge the Ministry of Education, Culture, Sport, Science and technology (MEXT) of Japan for the scholarship given me to study in Japan.

I would also thank to Ms. Natalya Shmakova and the lovely $E^3$ family for the great support, friendship, and advice.

To all the people I have failed to mention, thank you very much for the friendship, support, and help.

Finally, my deepest gratitude goes to my family for their unflagging love and unconditional support throughout my life and my studies. You made me live the most unique, magic and carefree childhood that have made me who I am.